

TANGLE ANALYSIS OF DIFFERENCE TOPOLOGY EXPERIMENTS: APPLICATIONS TO A MU PROTEIN-DNA COMPLEX

ISABEL K. DARCY, JOHN LUECKE, AND MARIEL VAZQUEZ

ABSTRACT. We develop topological methods for analyzing difference topology experiments involving 3-string tangles. Difference topology is a novel technique used to unveil the structure of stable protein-DNA complexes involving two or more DNA segments. We analyze such experiments for the Mu protein-DNA complex. We characterize the solutions to the corresponding tangle equations by certain knotted graphs. By investigating planarity conditions on these graphs we show that there is a unique biologically relevant solution. That is, we show there is a unique rational tangle solution, which is also the unique solution with small crossing number.

In [PJH], Pathania *et al* determined the shape of DNA bound within the Mu transposase protein complex using an experimental technique called difference topology [HJ, KBS, GBJ, PJH, PJH2, YJPH, YJH] and by making certain assumptions regarding the DNA shape. We show that their most restrictive assumption (the plectonemic form described near the end of section 1) is not needed, and in doing so, conclude that the only biologically reasonable solution for the shape of DNA bound by Mu transposase is the one they found [PJH] (Figure 0.1). We will call this 3-string tangle the PJH solution. The 3-dimensional ball represents the protein complex, and the arcs represent the bound DNA. The Mu-DNA complex modeled by this tangle is called the Mu transpososome

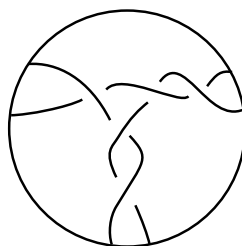


FIGURE 0.1

2000 *Mathematics Subject Classification.* 57M25; 92C40.

Key words and phrases. 3-string tangle, DNA topology, difference topology, Mu transpososome, graph planarity, Dehn surgery, handle addition lemma.

In section 1 we provide some biological background and describe eight difference topology experiments from [PJH]. In section 2, we translate the biological problem of determining the shape of DNA bound by Mu into a mathematical model. The mathematical model consists of a system of ten 3-string tangle equations (Figure 2.2). Using 2-string tangle analysis, we simplify this to a system of four tangle equations (Figure 2.15). In section 3 we characterize solutions to these tangle equations in terms of knotted graphs. This allows us to exhibit infinitely many different 3-string tangle solutions. The existence of solutions different from the PJH solution raises the possibility of alternate acceptable models. In sections 3 - 5, we show that all solutions to the mathematical problem other than the PJH solution are too complex to be biologically reasonable, where the complexity is measured either by the rationality or by the minimal crossing number of the 3-string tangle solution.

In section 3, we show that the only *rational* solution is the PJH solution. In particular we prove the following corollary.

Corollary 3.20. *Let \mathcal{T} be a solution tangle. If \mathcal{T} is rational or split or if \mathcal{T} has parallel strands, then \mathcal{T} is the PJH solution.*

In section 4 we show that any 3-string tangle with fewer than 8 crossings, up to free isotopy (*i.e.* allowing the ends of the tangle to move under the isotopy), must be either split or have parallel strands. Thus Corollary 3.20 implies that any solution \mathcal{T} different from the PJH solution must have at least 8 crossings up to free isotopy. Fixing the framing of a solution tangle (the normal framing of section 2), and working in the category of tangle equivalence – *i.e.* isotopy fixed on the boundary – we prove the following lower bound on the crossing number of exotic solutions:

Proposition 5.1. *Let \mathcal{T} be an in trans solution tangle. If \mathcal{T} has a projection with fewer than 10 crossings, then \mathcal{T} is the PJH tangle.*

The framing used in [PJH] is different than our normal framing. In the context of [PJH], Proposition 5.1 says that if Mu binds fewer than 9 crossings, then the PJH solution is the only solution fitting the experimental data. The PJH solution has 5 crossings. We interpret Corollary 3.20 and Proposition 5.1 as saying that the PJH solution is the only biologically reasonable model for the Mu transpososome.

Although we describe 8 experiments from [PJH], in the interest of minimizing lab time, we show that only 3 experiments (*in cis* deletion) are needed to prove the main result of sections 3 (Corollary 3.20) and 4. A fourth experiment (*in trans* deletion) allows us

to rule out some solutions (section 3) and is required for the analysis in section 5. The remaining four experiments (inversion) were used in model design [PJH].

The results in sections 2-4 extend to cases such as [YJPH, YJH] where the experimental products are $(2, L)$ torus links [HS] or the trefoil knot [KMOS]. The work in section 3 involves the analysis of knotted graphs as in [G], [ST], [T]. As a by-product, we prove the following:

Theorem 3.25. *Suppose \widehat{G} is a tetrahedral graph with the following properties:*

- (1) *There exists three edges e_1, e_2, e_3 such that $\widehat{G} - e_i$ is planar.*
- (2) *The three edges e_1, e_2, e_3 share a common vertex.*
- (3) *There exists two additional edges, b_{12} and b_{23} such that $X(\widehat{G} - b_{12})$ and $X(\widehat{G} - b_{23})$ have compressible boundary.*
- (4) *$X(\widehat{G})$ has compressible boundary.*

Then \widehat{G} is planar.

In subsection 3.4 we also give several examples of non-planar tetrahedral graphs to show that none of the hypothesis in Theorem 3.25 can be eliminated.

Acknowledgments

We would like to thank D. Buck, R. Harshey, S. Pathania, and C. Verjovsky-Marcotte for helpful comments. We would particularly like to thank M. Jayaram for many helpful discussions. We also thank M. Combs for numerous figures, R. Scharein and Knot-plot.com for assistance with Figure 1.8, and A. Stasiak, University of Lausanne, for the electron micrograph of supercoiled DNA in Figure 1.9.

J.L. would like to thank the Institute for Advanced Study in Princeton for his support as a visiting member. This research was supported in part by the Institute for Mathematics and its Applications with funds provided by the National Science Foundation (I.D. and M.V.); by a grant from the Joint DMS/NIGMS Initiative to Support Research in the Area of Mathematical Biology (NIH GM 67242) to I.D.; and by NASA NSCOR04-0014-0017, by MBRS SCORE S06 GM052588, and by NIH-RIMI Grant NMD000262 to M.V.

1. BIOLOGY BACKGROUND AND EXPERIMENTAL DATA

Transposable elements, also called mobile elements, are fragments of DNA able to move along a genome by a process called transposition. Mobile elements play an important role in the shaping of a genome [DMBK, S], and they can impact the health of an organism by

introducing genetic mutations. Of special interest is that transposition is mechanistically very similar to the way certain retroviruses, including HIV, integrate into their host genome.

Bacteriophage Mu is a system widely used in transposition studies due to the high efficiency of Mu transposase (reviewed in [CH]). The MuA protein performs the first steps required to transpose the Mu genome from its starting location to a new DNA location. MuA binds to specific DNA sequences which we refer to as attL and attR sites (named after *Left* and *Right* attaching regions). A third DNA sequence called the enhancer (E) is also required to assemble the Mu transpososome. The Mu transpososome is a very stable complex consisting of 3 segments of double-stranded DNA captured in a protein complex [BM, MBM]. In this paper we are interested in studying the topological structure of the DNA within the Mu transpososome.

1.1. Experimental design. We base our study on the difference topology experiments of [PJH]. In this technique, circular DNA is first incubated with the protein(s)¹ under study (in this case, MuA), which bind DNA. A second protein whose mechanism is well understood is added to the reaction (in this case Cre). This second protein is a protein that can cut DNA and change the circular DNA topology before resealing the break(s), resulting in knotted or linked DNA. DNA crossings bound by the first protein will affect the product topology. Hence one can gain information about the DNA conformation bound by the first protein by determining the knot/link type of the DNA knots/links produced by the second protein.

In the experiments, first circular unknotted DNA is created containing the three binding sites for the Mu transpososome (attL, attR, E) and two binding sites for Cre (two *loxP* sites). We will refer to this unknotted DNA as *substrate*. The circular DNA is first incubated with the proteins required for Mu transposition, thus forming the transpososome complex. This complex leaves three DNA loops free outside the transpososome (Figure 1.1). The two *loxP* sites are strategically placed in two of the three outside loops. The complex is incubated with Cre enzymes, which bind the *loxP* sites, introduce two double-stranded breaks, recombine the loose ends and reseal them. A possible 2-string tangle model for the local action of Cre at these sites is shown in Figure 1.2 [GGD]. This

¹Although we use the singular form of protein instead of the plural form, most protein-DNA complexes involve several proteins. For example formation of the Mu transpososome involves four MuA proteins and the protein HU. Also since these are test tube reactions and not single molecule experiments, many copies of the protein are added to many copies of the DNA substrate to form many complexes.

cut-and-paste reaction may change the topology (knot/link type) of the DNA circle. Changes in the substrate's topology resulting from Cre action can reveal the structure within the Mu transpososome.

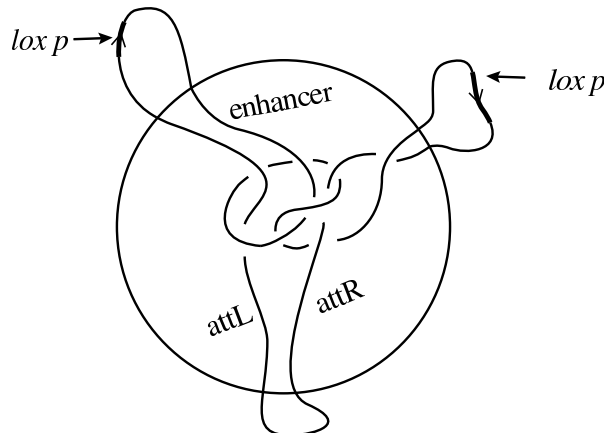


FIGURE 1.1

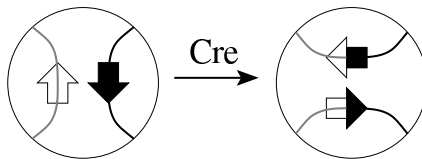


FIGURE 1.2

By looking at such topological changes, Pathania *et al.* [PJH] deduced the structure of the transpososome to be the that of Figure 0.1 (the *PJH solution*). In this paper we give a knot theoretic analysis that supports this deduction. We show that although there are other configurations that would lead to the same product topologies seen in the experiments, they are necessarily too complicated to be biologically reasonable.

If the orientation of both *loxP* sites induces the same orientation on the circular substrate (in biological terms, the sites are *directly repeated*), then recombination by Cre results in a link of two components and is referred to as a *deletion* (Figure 1.3, left). Otherwise the sites are *inversely repeated*, the product is a knot, and the recombination is called an *inversion* (Figure 1.3, right).

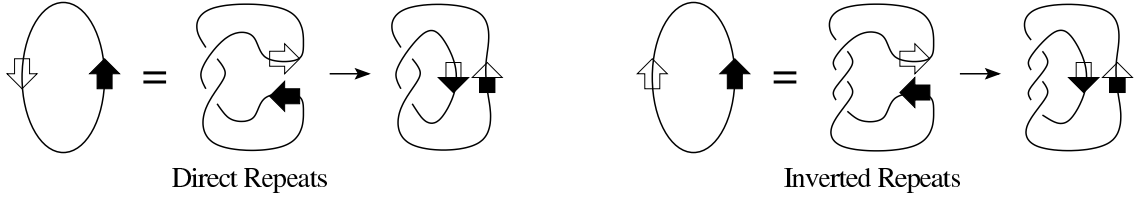


FIGURE 1.3

In [PJH] six out of eight experiments were designed by varying the relative positions of the *loxP* sites and their relative orientations. The last pair of experiments involved omitting one of the Mu binding sites on the circular substrate and placing that site on a linear piece of DNA to be provided “*in trans*” as described below.

In the first pair of experiments from [PJH], *loxP* sites were introduced in the substrate on both sides of the enhancer sequence (E) (Figure 1.1). The sites were inserted with orientations to give, in separate runs, deletion and inversion products. The transpososome was disassembled and the knotted or linked products analyzed using gel electrophoresis and electron microscopy. The primary inversion products were (+) trefoils, and the primary deletion products were 4-crossing right-hand torus links ((2, 4) torus links).

The assay was repeated, but now the *loxP* sites were placed on both sides of the attL sequence. The primary products were (2, 4) torus links for deletion, and trefoils for inversion. In a third set of experiments, the assay was repeated again with the *loxP* sites on both sides of the attR sequence. The primary products were (2, 4) torus links for deletion, and 5-crossing knots for inversion.

Recall that in these first six experiments, the three Mu binding sites, attL, attR, and the enhancer, are all placed on the same circular DNA molecule. We will refer to these six experiments as the *in cis* experiments to differentiate them from the final set of experiments, the *in trans* assay. In the *in trans* assay, circular DNA substrates were created that contained attL and attR sites but no enhancer site. Each *loxP* site was inserted between the attL and attR sites as shown in Figure 1.4. The enhancer sequence was placed on a linear DNA molecule. The circular substrate was incubated in solution with linear DNA molecules containing the enhancer sequence and with the proteins required for transpososome assembly. In this case, we say that the enhancer is provided *in trans*. The *loxP* sites in the resulting transpososome complex underwent Cre recombination. After the action of Cre and the disassembly of the transpososome

(including the removal of the loose enhancer strand), the primary inversion products were trefoil knots, and the primary deletion products were (2,2) torus links (Hopf links).

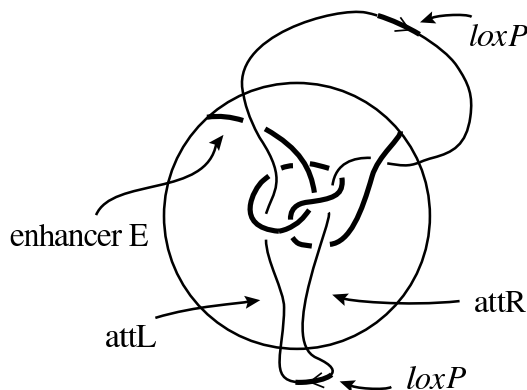


FIGURE 1.4

The results of these experiments are summarized in Table 1.5². Vertical columns correspond to the placement of *loxP* sites, *e.g.* the attL column shows inversion and deletion products when the *loxP* sites were placed on both sides of the attL sequence.

	enhancer	attL	attR	<i>in trans</i>
Inversion	(+)-trefoil	trefoil	5-crossing knot	trefoil
Deletion	(2, 4)-torus link	(2, 4)-torus link	(2, 4)-torus link	(2, 2)-torus link

Table 1.5

1.2. Tangle Model. Tangle analysis is a mathematical method that models an enzymatic reaction as a system of tangle equations [ES1, SECS]. 2-string tangle analysis has been successfully used to solve the topological mechanism of several site-specific recombination enzymes [ES1, ES2, SECS, GBJ, D, VS, VCS, BV]. The Mu transpososome is better explained in terms of 3-string tangles. Some efforts to classifying rational 3-string tangles and solving 3-string tangle equations are underway [C1, C2, EE, D1]. In this paper we find tangle solutions for the relevant 3-string tangle equations; we characterize

²The chirality of the products was only determined when the *loxP* sites were placed on both sides of the enhancer sequence. We here assume the chirality in Table 1.5, where (2,4) torus link denotes the 4-crossing right-hand torus link. If any of the products are left-hand (2, 4) torus links, the results of sections 2 - 5 applied to these products leads to biologically unlikely solutions.

solutions in terms of certain knotted graphs called solution graphs and show that the PJH solution (Figure 0.1) is the unique rational solution.

The unknotted substrate captured by the transpososome is modeled as the union of the two 3-string tangles $\mathcal{T}_0 \cup \mathcal{T}$, where \mathcal{T} is the transpososome tangle and \mathcal{T}_0 is the tangle outside the transpososome complex. $\mathcal{T}_0 \cup \mathcal{T}$ is represented in Figure 1.1. Notice that in this figure the *loxP* sites are placed on both sides of the enhancer sequence, but the placement of these sites varies throughout the experiments.

Figure 1.6 shows the action of Cre on the transpososome proposed in [PJH]. The experimentally observed products are indicated in this figure. For example, *E*-inversion refers to the product corresponding to inversely repeated *loxP* sites introduced on both sides of the enhancer sequence. However, there are other 3-string tangles, assuming the same action of Cre, that give rise to the same products. Figures 1.7 and 1.8 show two such examples. If one replaces the tangle of Figure 0.1 with either that of Figure 1.7 or 1.8 in Figure 1.6, the captions remain valid.

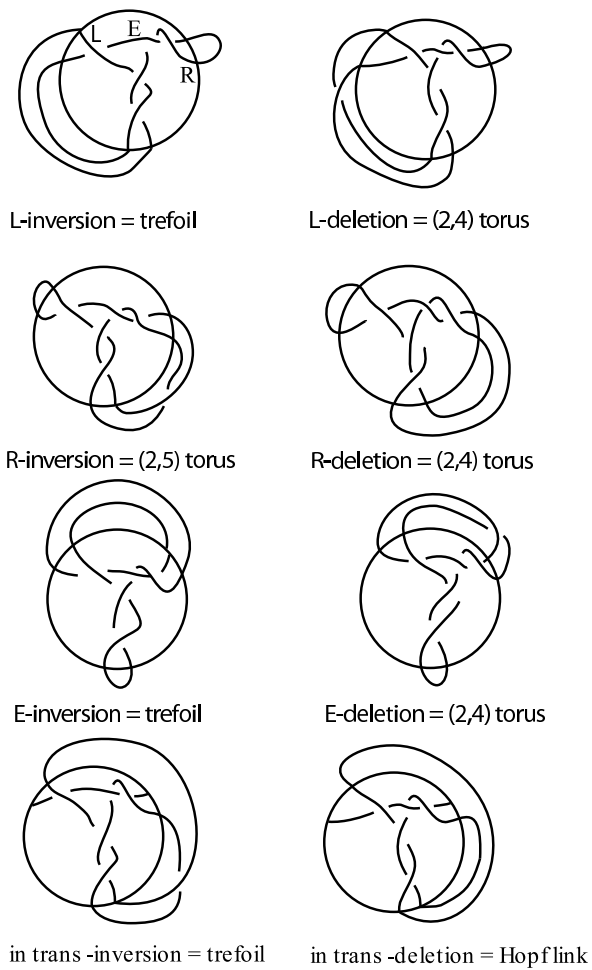


FIGURE 1.6

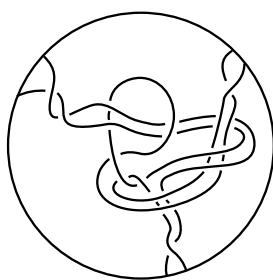


FIGURE 1.7

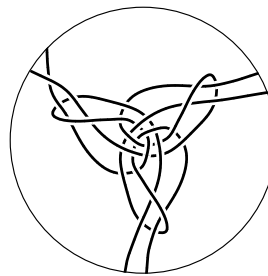


FIGURE 1.8

[PJH] determined the shape of DNA within the Mu transpososome to be the PJH solution (Figure 0.1) by making a restrictive assumption regarding this DNA conformation. They looked at only the most biologically likely shape: a 3-branched supercoiled

structure like that shown in Figure 1.9³. The *loxP* sites were strategically⁴ placed close to the Mu transpososome binding sites in order to prevent Cre from trapping random crossings not bound within the Mu transpososome. In half the experiments it was assumed that Cre trapped one extra crossing outside of the Mu transpososome in order to obtain the *loxP* sequence orientation of Figure 1.2 (indicated by the arrows). It was also assumed that this occurred with the higher crossing product when comparing inversion versus deletion products. Hence a crossing outside of the Mu transpososome can be seen in Figure 1.6 in the case of E-deletion, L-deletion, R-inversion, and *in trans* inversion. In all other cases, it was assumed that Cre did not trap any extra crossings outside of the Mu transpososome. By assuming a branched supercoiled structure, [PJH] used their experimental results to determine the number of crossings trapped by Mu in each of the three branches. In sections 2–5 we show that we are able to reach the same conclusion as [PJH] without assuming a branched supercoiled structure within the Mu transpososome.

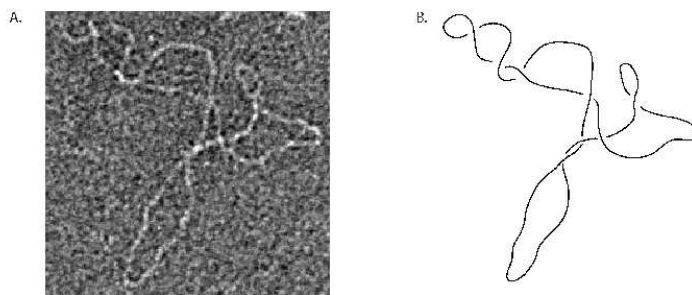


FIGURE 1.9

2. NORMAL FORM

2.1. Normal form. The substrate for Cre recombination in [PJH] is modeled as the 3-string tangle union $\mathcal{T} \cup \mathcal{T}_0$. We here introduce a framing for \mathcal{T} called the normal form, which is different from that in the PJH solution (section 1). The choice of framing affects only the arithmetic in section 2 and does not affect any of the results in sections 3 or 4. The results of section 5 on the crossing number of \mathcal{T} are made with respect to this framing.

In Figure 2.1, let c_1, c_2, c_3 be the strings of \mathcal{T}_0 and s_{12}, s_{23}, s_{31} be the strings of \mathcal{T} . The substrate is the union of the c_i 's and the s_{ij} 's. We assume there is a projection of $\mathcal{T} \cup \mathcal{T}_0$

³Electron microscopy of supercoiled DNA courtesy of Andrzej Stasiak.

⁴Although we described only 8 experiments from [PJH], they performed a number of experiments to determine and check effect of site placement.

so that c_1, c_2, c_3 are isotopic (relative endpoints) onto the tangle circle and so that the endpoints of s_{ij} are contiguous on the tangle circle (Figure 2.1). Note that this projection is different from that in [PJH]. It is a simple matter to convert between projections, as described below.

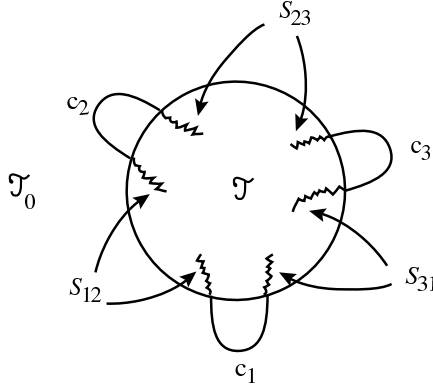
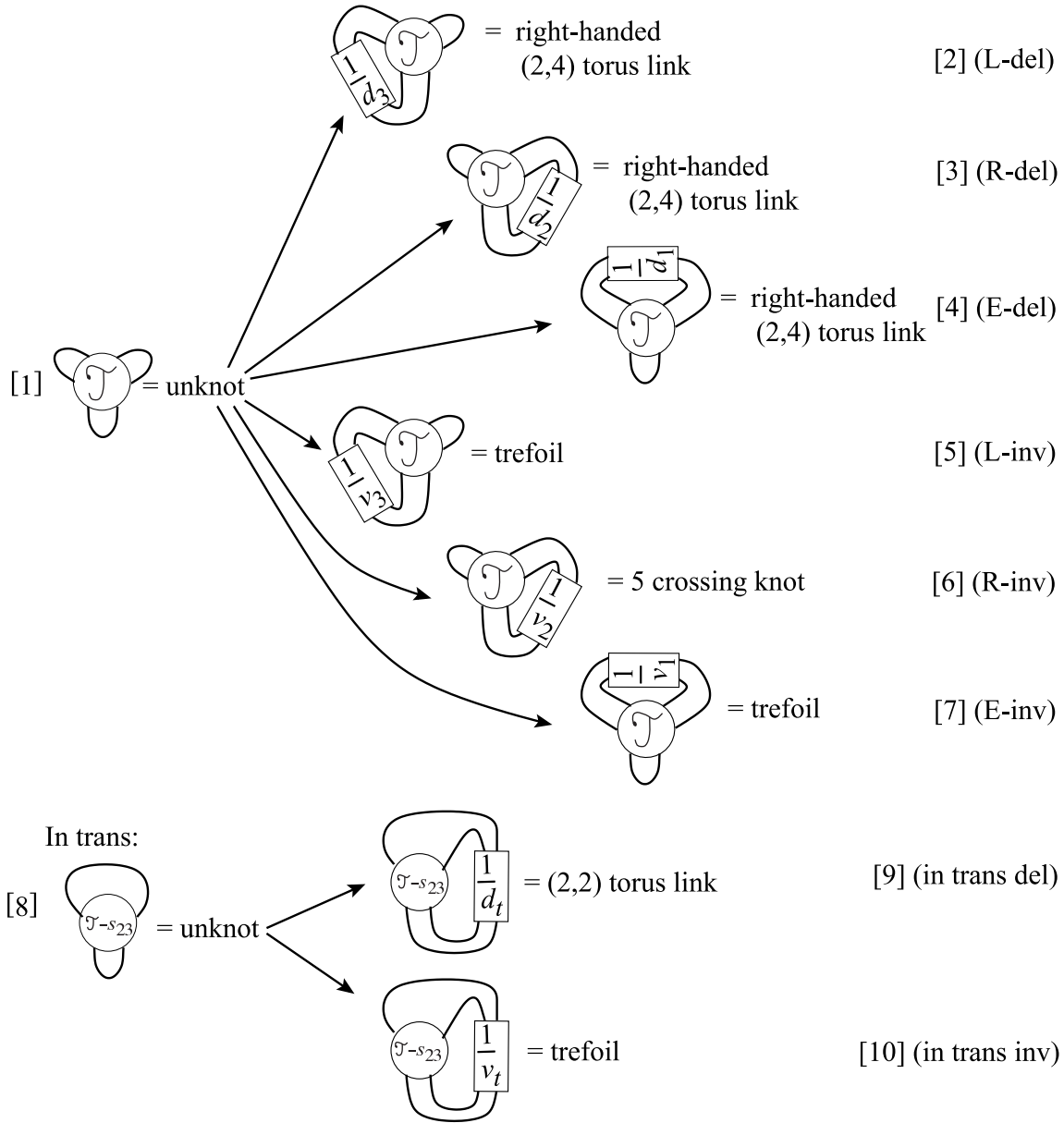


FIGURE 2.1

In each experiment the two recombination sites for Cre (*loxP* sites) are located on two strings c_i and c_j ($i \neq j$). Cre bound to a pair of strings $c_i \cup c_j$ can be modeled as a 2-string tangle P of type $\frac{0}{1}$. Earlier studies of Cre support the assumption that Cre recombination takes $P = \frac{0}{1}$ into $R = \frac{1}{0}$, where for both tangles, the Cre binding sites are in anti-parallel orientation (Figure 1.2) [PJH, GBJ, GGD, KBS]. Note that from a 3-dimensional point of view, the two sites can be regarded as parallel or anti-parallel as we vary the projection [SECS, VCS, VDL]. With our choice of framing any Cre-DNA complex formed by bringing together two *loxP* sites (*e.g.* strings c_i and c_j) results in $P = (0)$ with anti-parallel sites when the *loxP* sites are directly repeated. Furthermore, it is possible that Cre recombination traps crossings outside of the Mu and Cre protein-DNA complexes. For mathematical convenience we will enlarge the tangle representing Cre to include these crossings which are not bound by either Mu or Cre but are trapped by Cre recombination. That is, the action of Cre recombination on $c_i \cup c_j$ will be modeled by taking $P = \frac{0}{1}$ into $R = \frac{1}{d}$ for some integer d . Hence the system of tangle equations shown in Figure 2.2 can be used to model these experiments where the rational tangles $\frac{1}{d_i}, \frac{1}{v_i}, \frac{1}{d_i}, \frac{1}{v_t}$ represent non-trivial topology trapped inside R by Cre recombination, but not bound by Mu. The tangle \mathcal{T} , representing the transpososome (*i.e.* the Mu-DNA complex), is assumed to remain constant throughout the recombination event [SECS, PJH]. Recall that the first six experiments where the three Mu binding sites, attL, attR, and the enhancer, are all placed on the same circular DNA molecule will be referred to as the

in cis experiments. The remaining two experiments will be referred to as the *in trans* experiments since the enhancer sequence is provided *in trans* on a linear DNA molecule separate from the circular DNA molecule containing the attL and attR sites. The tangle equation (1) in Figure 2.2 corresponds to the unknotted substrate equation from the first six experiments. Equations (2)-(4) correspond to three product equations modeling the three *in cis* deletion experiments, while equations (5)-(7) correspond to the three product equations modeling the three *in cis* inversion experiments. Equation (8) corresponds to the unknotted substrate equation for the two *in trans* experiments, while equations (9) and (10) correspond to the product equations modeling *in trans* deletion and *in trans* inversion, respectively. In addition to modeling experimental results in [PJH], these equations also model results in [PJH2, YJH].



where $P =$ or , $n_i + n_j = n$; and $R =$ if $n=0$, or $R = \frac{1}{n} =$ if $n>0$, or $R =$ if $n<0$

FIGURE 2.2

Figure 2.1 partially defines a framing for the tangle \mathcal{T} . One can go further by specifying values for d_1, d_2, d_3 for the three *in cis* deletion experiments. We define the *normal form equations* to be the system of equations (1) - (4) in Figure 2.2 (corresponding to the *in cis* deletion experiments) with the additional requirement that $d_1 = d_2 = d_3 = 0$. We focus first on these four equations as only the *in cis* deletion experiments are needed for our main results; but the other experiments were important experimental controls and were used by [PJH] to determine the tangle model for the Mu transpososome.

Definition 1. A 3-string tangle \mathcal{T} is called a *solution tangle* iff it satisfies the four normal form equations.

Note that in the normal form equations, the action of Cre results in replacing $P = c_i \cup c_j = \frac{0}{1}$ with $R = \frac{1}{0}$ for the three *in cis* deletion experiments. If we wish to instead impose a framing where $P = c_i \cup c_j = 0/1$ is replaced by $R = \frac{1}{d_k}$ for given d_k , $k = 1, 2, 3$, we can easily convert between solutions. Suppose \mathcal{T} is a solution to this non-normal form system of equations. We can move n_i twists from R into \mathcal{T} at c_i , for each i where $n_i + n_j = d_k$ (Figure 2.3). Hence \mathcal{T} with n_i crossings added inside \mathcal{T} at c_i for each i is a solution tangle (for the normal form equations). Note the n_i are uniquely determined. Similarly, if \mathcal{T} is a solution tangle (for the normal form equations), then for given d_k we can add $-n_i$ twists to \mathcal{T} at c_i to obtain a solution to the non-normal form equations.

Remark. For biological reasons [PJH] chose $d_1 = -1$, $d_2 = 0$, $d_3 = -1$. Hence $n_1 = 0$, $n_2 = -1$, $n_3 = 0$. This corresponds to adding a right-hand twist at c_2 to a solution in the PJH convention (such as Figure 0.1) to obtain a solution tangle (such as Figure 2.4). Conversely, by adding a single left-hand twist at c_2 to a solution tangle, we get the corresponding solution in the PJH convention (e.g. from the solution tangle of Figure 2.4 to the PJH solution of Figure 0.1).

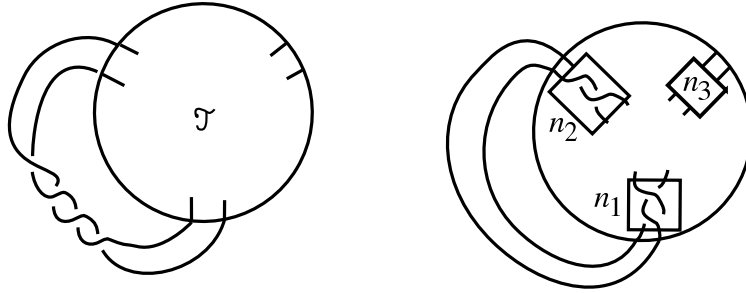


FIGURE 2.3

Remark. We will show that knowing the number of crossings trapped by Cre outside of the Mu transpososome in the three *in cis* deletion experiments is sufficient for determining the number of crossings trapped outside the Mu transpososome in all experiments. In other words choosing d_1, d_2, d_3 determines v_1, v_2, v_3, v_t , and d_t .

Next we apply traditional 2-string tangle calculus [ES1] to the equations arising from the *in cis* deletion experiments.

2.2. The three *in cis* deletion tangle equations. With abuse of the c_i notation of Figure 2.1, let the tangle circle be the union of arcs $c_1 \cup x_{12} \cup c_2 \cup x_{23} \cup c_3 \cup x_{31}$ (Figure 2.4). We think of these arcs as providing a framing for the tangle \mathcal{T} .

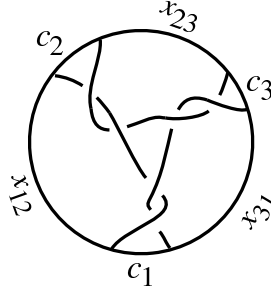


FIGURE 2.4

Let $O_i = \mathcal{T} \cup c_i$ be the 2-string tangle obtained by capping off $s_{ji} \cup s_{ik}$ with c_i . Then s_{kj} is one of the strings of the 2-string tangle O_i , let \hat{s}_i denote the other (Figure 2.5)

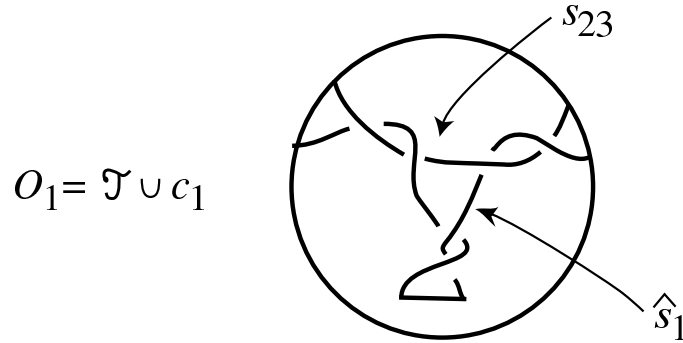


FIGURE 2.5

By capping \mathcal{T} along each c_i , we approach the problem of finding all possible 3-string tangles for the Mu transpososome by first solving three systems of two 2-string tangle equations (one for each c_i). Figure 2.6 illustrates the definitions of 2-string tangle addition (+) and numerator closure (N). Figure 2.7 shows a system of two 2-string tangle equations arising from Cre recombination on the Mu transpososome. $\mathcal{T} \cup c_2$ is represented by the

blue and green 2-string tangle while the smaller pink 2-string tangle represents Cre bound to *loxP* sites before (left) and after (right) recombination.

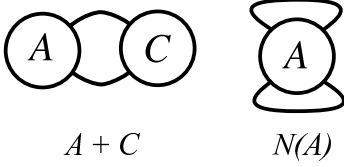


FIGURE 2.6

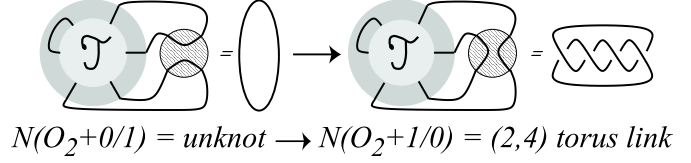


FIGURE 2.7

Lemma 2.1. (*in cis deletion*) Let \mathcal{T} be a solution tangle. That is, consider the three *in cis deletion experiments* which convert unknotted substrates to right-hand $(2, 4)$ torus links. Let $O_i = \mathcal{T} \cup c_i$ be the 2-string tangle obtained by capping \mathcal{T} along c_i . Then O_i is the $-1/4$ tangle, $i = 1, 2, 3$.

Proof. All the *in cis deletion* events, modeled by replacing $P = c_j \cup c_k = \frac{0}{1}$ by $R = \frac{1}{0}$ in normal form (see Figure 2.8), lead to identical systems of two 2-string tangle equations:

$$\begin{aligned} N(O_i + \frac{0}{1}) &= \text{unknot} \\ N(O_i + \frac{1}{0}) &= (2, 4) \text{ torus link} \end{aligned}$$

By [HS], O_i is a rational tangle. By tangle calculus, the system admits a unique solution $O_i = -1/4$, $i = 1, 2, 3$ [ES1] (see also [D, VCS]).

□

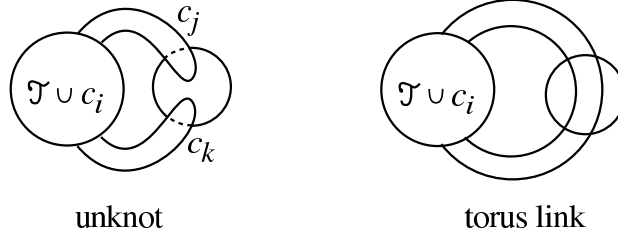


FIGURE 2.8

2.3. The three *in cis* inversion tangle equations. Each Cre inversion experiment is also modeled as a system of tangle equations:

$$\begin{aligned} N(O_i + \frac{0}{1}) &= \text{unknot} \\ N(O_i + \frac{1}{v_i}) &= \text{inversion product} \end{aligned}$$

If we assume that the DNA-protein complex is constant for each pair of deletion/inversion experiments, then by Lemma 2.1, $O_1 = O_2 = O_3 = -1/4$. If the inversion products are

known, v_i , $i = 1, 2, 3$, can be determined by tangle calculus. From [PJH] we assume that both L-inversion and E-inversion produce the (+)trefoil. Also R-inversion produces a 5-crossing knot (see Table 1.5), which must be a 5-torus knot since $O_2 = -1/4$. We assume this is the (+)5-torus knot, for if it were the (-)5-torus knot then $v_2 = 9$ which is biologically unlikely. Hence the only biologically reasonable solutions to the inversion equations, with $O_i = -1/4$, $i = 1, 2, 3$ are:

$$\begin{aligned}
 (2.1) \quad & \text{L-inversion, } P = \frac{0}{1} \text{ and } R = \frac{1}{1}, \text{ product } = (+)\text{trefoil;} \\
 & \text{R-inversion, } P = \frac{0}{1} \text{ and } R = \frac{-1}{1}, \text{ product } = (+)\text{5-torus knot;} \\
 & \text{E-inversion, } P = \frac{0}{1} \text{ and } R = \frac{1}{1}, \text{ product } = (+)\text{trefoil}
 \end{aligned}$$

Other possible solutions exist if O_i is allowed to change with respect to the deletion *versus* inversion experiments. However, it is believed that the orientation of the Cre binding sites (inverted versus direct repeats, Figure 1.3) does not affect the transpososome configuration.

2.4. Linking number considerations. In Lemma 2.2 we compute linking numbers related to the deletion experiments.

Assume \mathcal{T} is a solution tangle. First, let \hat{x}_i be the arc on the tangle circle given by $x_{ji} \cup c_i \cup x_{ik}$. We compute the linking number between $x_{jk} \cup s_{jk}$ and $\hat{s}_i \cup \hat{x}_i$, using the orientation induced from the tangle circle into each component and using the sign convention in Figure 2.9. The linking number quantifies the pairwise interlacing of arcs after capping off.

Second, we compute the linking number of $x_{ij} \cup s_{ij}$ and $x_{ki} \cup s_{ki}$, with sign and orientation conventions as before. This linking number calculation quantifies the interlacing between any two arcs in \mathcal{T} .

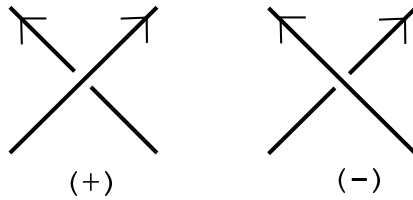


FIGURE 2.9

Lemma 2.2. Assume \mathcal{T} is a solution tangle. Then

$$\begin{aligned} \ell k(x_{jk} \cup s_{jk}, \hat{s}_i \cup \hat{x}_i) &= -2 \\ \ell k(x_{ij} \cup s_{ij}, x_{ki} \cup s_{ki}) &= -1 \end{aligned} \quad \{i, j, k\} = \{1, 2, 3\}$$

Proof. The first equation follows from Lemma 2.1.

To get the second equation we note that $\hat{s}_i \cup \hat{x}_i$ can be obtained via a banding connecting $x_{ij} \cup s_{ij}$ with $x_{ki} \cup s_{ki}$ along c_i as indicated in Figure 2.10.

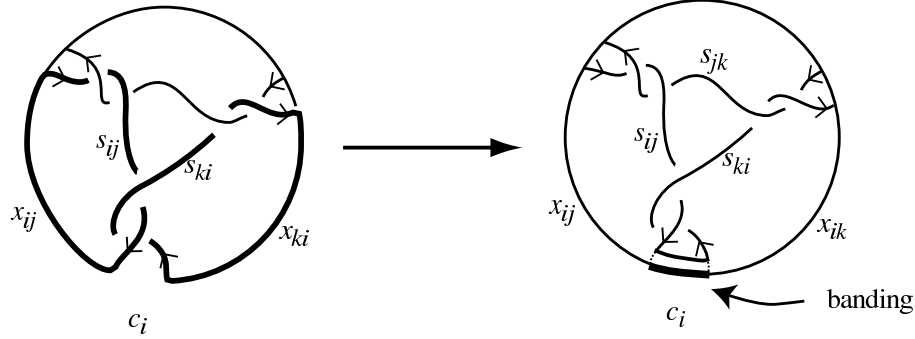


FIGURE 2.10

Then for $\{i, j, k\} = \{1, 2, 3\}$,

$$-2 = \ell k(x_{jk} \cup s_{jk}, \hat{s}_i \cup \hat{x}_i) = \ell k(x_{jk} \cup s_{jk}, x_{ij} \cup s_{ij}) + \ell k(x_{jk} \cup s_{jk}, x_{ki} \cup s_{ki}) .$$

Solving three equations ($\{i, j, k\} = \{1, 2, 3\}$), we obtain $\ell k(x_{ij} \cup s_{ij}, x_{jk} \cup s_{jk}) = -1$. \square

In the next section we will see how the *in cis* deletion results extend to the analysis of the remaining experiments (*in trans* deletion and inversion).

2.5. *In trans* experiments. In the *in trans* portion of [PJH] (described in section 1) the enhancer sequence is not incorporated into the circular DNA substrate; it remains separate in solution on its own linear molecule when the transpososome is formed (Figure 2.11). Assuming the transpososome complex forms the same 3-string tangle in this context, the transpososome writes the substrate as a union of two 2-string tangles: \mathcal{T}'_0 , a trivial tangle outside the transpososome; and $\mathcal{T}' = \mathcal{T} - s_{23}$, the tangle formed by the *attR* and *attL* strands (where s_{23} is the enhancer strand in \mathcal{T}).



FIGURE 2.11

Lemma 2.3. (*in trans deletion*) Let \mathcal{T} be a solution tangle. Suppose \mathcal{T} also satisfies equations (8) and (9) in Figure 2.2 where d_t is as shown in this figure. Then $d_t = 0, 4$ and $\mathcal{T} - s_{23} = \frac{1}{-2}$.

Proof. When Cre acts on the *loxP* sites in the *in trans* experiment, we assume that it takes the $\frac{0}{1}$ tangle to $\frac{1}{d_t}$ (Figure 2.12). The Cre deletion product *in trans* is a Hopf link (*i.e.* a $(2, 2)$ torus link). Hence we are solving the 2-string tangle equations, $N((\mathcal{T} - s_{23}) + \frac{0}{1}) = \text{unknot}$, $N((\mathcal{T} - s_{23}) + \frac{1}{d_t}) = (2, 2)$ torus link. By [BL] $\mathcal{T} - s_{23}$ is rational, and by tangle calculus [ES1], $\mathcal{T} - s_{23} = \frac{1}{\pm 2 - d_t}$, which implies that $\ell k(x_{31} \cup s_{31}, x_{12} \cup s_{12}) = \frac{\pm 2 - d_t}{2}$. By Lemma 2.2, $\ell k(x_{31} \cup s_{31}, x_{12} \cup s_{12}) = -1$. Hence $\frac{\pm 2 - d_t}{2} = -1$. Thus $d_t = 0, 4$ and $\mathcal{T} - s_{23} = \frac{1}{-2}$. \square

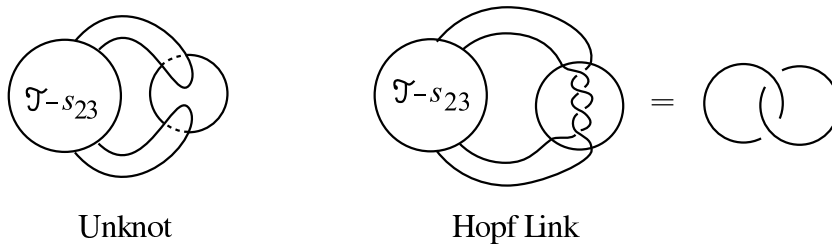


FIGURE 2.12

Remark. (*In trans inversion*) If $\mathcal{T} - s_{23} = \frac{1}{-2}$, then the *in trans* Cre inversion product is $N(\mathcal{T} - s_{23} + \frac{1}{v_t}) = N(\frac{1}{-2} + \frac{1}{v_t}) = (2, 2 - v_t)$ torus knot. A $(2, 3)$ torus knot (*i.e.* the trefoil) *in trans* inversion product implies $v_t = -1$.

2.6. Summary. The next proposition summarizes the results in this section.

Proposition 2.4. *Let \mathcal{T} be a solution tangle which also satisfies the in trans deletion experiments, and let s_{23} correspond to the enhancer strand in the [PJH] experiments. Then*

$$(2.2) \quad O_i = \mathcal{T} \cup c_i = -\frac{1}{4}, \quad \mathcal{T} - s_{23} = -\frac{1}{2}$$

The in trans deletion reaction of Cre is modeled by replacing $c_1 \cup (c_2 \cup x_{23} \cup c_3) = \frac{0}{1}$ by the $\frac{1}{0}$ or $\frac{1}{4}$ tangle (i.e. $d_t = 0, 4$, see Figure 2.14).

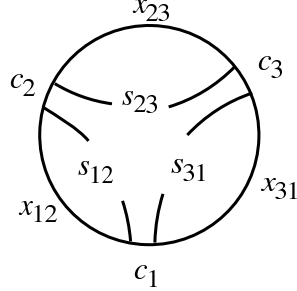


FIGURE 2.13

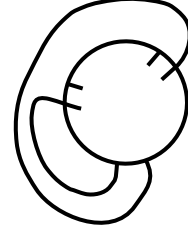


FIGURE 2.14

Remark. In declaring $O_i = -1/4$ we are using the framing coordinate of the tangle circle with $c_j \cup c_k = 0/1, x_{jk} \cup \hat{x}_i = 1/0$.

Proposition 2.4 can be generalized to products of deletion that are $(2, L_i)$ torus links, and a $(2, L_t)$ torus link for the *in trans* experiment:

Proposition 2.5. *Let \mathcal{T} satisfy equations (1)-(4), (8)-(9) of Figure 2.2 except that the in cis deletion experiments produce $(2, L_i)$ torus links, $L_i \neq \pm 2$, for $i = 1, 2, 3$ and the in trans deletion experiment results in a $(2, L_t)$ torus link. Assume $d_1 = d_2 = d_3 = 0$ and that s_{23} corresponds to the enhancer strand. Then*

$$(2.3) \quad O_i = \mathcal{T} \cup c_i = -\frac{1}{L_i}, \quad \mathcal{T} - s_{23} = \frac{1}{\frac{L_2+L_3-L_1}{2}}.$$

If $|L_t| = 2$, then $d_t = \frac{-L_j+L_i+L_k \pm 4}{2}$. If $|L_t| \neq 2$, then $d_t = \frac{-L_j+L_i+L_k-2L_t}{2}$.

Note similar results hold if $L_i = \pm 2$ for $i = 1, 2$, and/or 3, but as this breaks into cases, we leave it to the reader.

Remark. Sections 3 and 4 rely on the fact the tangles in Figure 2.15 are all of the form $\frac{1}{m_i}$. This would still be the case no matter the choice of framing (discussed at the beginning of this section) or the type of the $(2, L_i)$ torus link products. Hence the results of sections 3 and 4 apply more generally.

Note that a 3-string tangle \mathcal{T} is a solution tangle iff it satisfies the condition $O_i = \mathcal{T} \cup c_i = -\frac{1}{4}$ for $i = 1, 2, 3$ (see Definition 1 and Lemma 2.1). This corresponds to the first three equations in Figure 2.15. The main result in section 3 (Corollary 3.20) only depends on the three *in cis* deletion experiments.

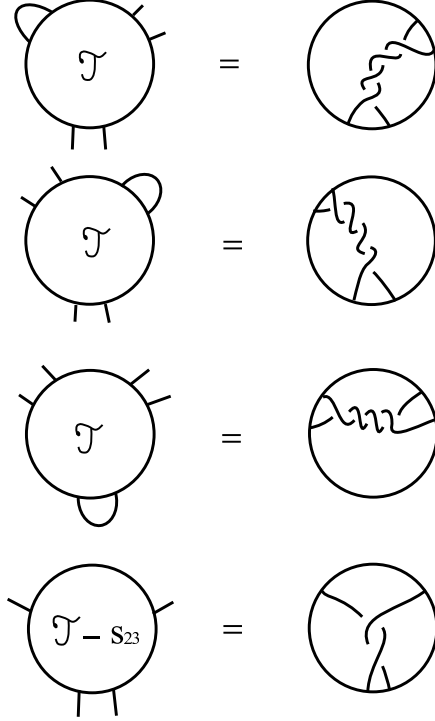


FIGURE 2.15

If in addition a solution tangle satisfies the *in trans* deletion equation, then we call it an *in trans solution tangle*:

Definition 2. A 3-string tangle \mathcal{T} is called an *in trans solution tangle* iff it satisfies Equation 2.2 of Proposition 2.4. This is equivalent to a tangle satisfying all the equations of Figure 2.15.

Note: **Proposition 2.4 reduces the study of transpososome tangles to that of *in trans* solution tangles.** In section 3 we classify solution tangles in terms of solution graphs and use this to show that the only solution tangle (and hence the only *in trans* solution tangle) that is rational is the PJH tangle.

Remark. The proof of Propositions 2.4 and 2.5 use the deletion products only. As the remaining analysis depends only on Proposition 2.4, we see that the inversion products

are unnecessary for our analysis. However, the inversion products were used to determine the framing in [PJH].

3. SOLUTION GRAPHS

In sections 3.1 and 3.2 we relate solution tangles to wagon wheel graphs and tetrahedral graphs. We use wagon wheel graphs to find an infinite number of solution tangles in section 3.1. Recall by Definition 1 that a solution tangle is a 3-string tangle satisfying the three *in cis* deletion equations (*i.e.*, $O_i = \mathcal{T} \cup c_i = -\frac{1}{4}$ for $i = 1, 2, 3$ in Equation 2.2 of Proposition 2.4; first three equations of Figure 2.15), while by Definition 2, an *in trans* solution tangle is a solution tangle which also satisfies the *in trans* deletion equation $\mathcal{T} - s_{23} = -\frac{1}{2}$. In section 3.3 we show that the only rational solution tangle is the PJH tangle. In section 3.5, we extend this result to tangles which are split or have parallel strands using results in section 3.4 regarding the exterior of a solution graph. In section 3.6, we show that if a solution tangle is also an *in trans* solution tangle, then its exterior is a handlebody. We use this in section 3.7 to investigate the planarity of tetrahedral graphs.

3.1. Solution tangles are carried by solution graphs.

Definition 3. A 3-string tangle is *standard* iff it can be isotoped rel endpoints to Figure 3.1. A standard tangle with $n_i = -2$ is called the *PJH tangle*.

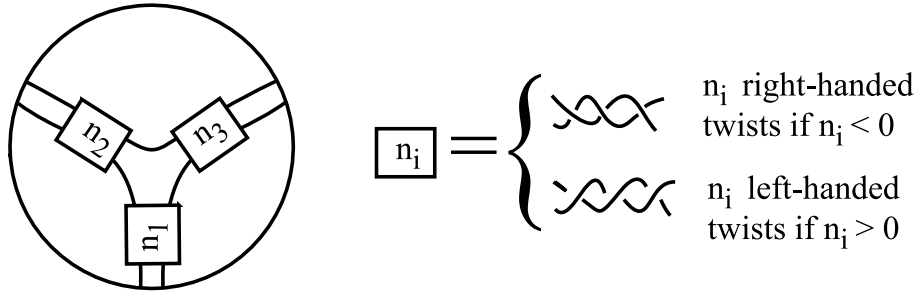


FIGURE 3.1

Lemma 3.1. *If a solution tangle is standard, then it is the PJH tangle.*

Proof. Write and solve the three equations, $n_i + n_j = -4$, describing the integral tangles resulting from capping along individual c_k . \square

Lemma 3.2. *If an in trans solution tangle is standard, then it is the PJH tangle.*

Proof. By Lemma 3.1, since an *in trans* solution tangle is also a solution tangle. \square

Remark. The assumption in [PJH] of the branched supercoiled structure (see the end of section 1) is equivalent to assuming the *in trans* solution tangle is standard. In that paper, the authors deduced the transpososome configuration with a method similar to that of Lemma 3.1. The PJH solution thus obtained is equivalent to our PJH tangle when normal framing is imposed.

Definition 4. The *abstract wagon wheel* is the graph of Figure 3.2. The vertices are labelled v_1, v_2, v_3 ; the edges labelled $e_1, e_2, e_3, b_{12}, b_{23}, b_{31}$. A *wagon wheel graph*, G , is a proper embedding of the abstract wagon wheel into B^3 with the endpoints of the e_i in the 10, 2, and 6 o'clock positions on the tangle circle (e.g. Figure 3.3). Two wagon wheel graphs are the *same* if there is an isotopy of B^3 , which is fixed on ∂B^3 , taking one graph to the other.

Definition 5. If a properly embedded graph lies in a properly embedded disk in the 3-ball, we call it *planar*.

Figure 3.4 gives examples of planar and non-planar wagon wheel graphs. Note that the non-planar graph in Figure 3.4 contains the knotted arc $e_2 \cup b_{23} \cup e_3$. The disk in which a planar wagonwheel lies may be taken to be the one given by the plane of the page, whose boundary is the tangle circle.

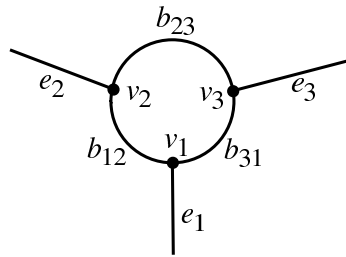


FIGURE 3.2

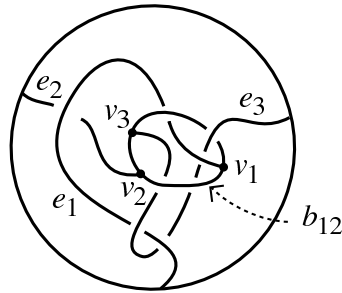


FIGURE 3.3

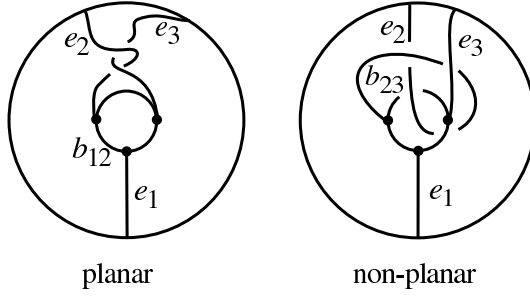


FIGURE 3.4

Definition 6. Let G be a wagon wheel graph, and let $N(G)$ denote a regular neighborhood of G in the 3-ball. Let $\mathcal{J}_1, \mathcal{J}_2, \mathcal{J}_3$ be meridian disks of $N(G)$ corresponding to edges e_1, e_2, e_3 . Let $J_i = \partial \mathcal{J}_i$. Let $\Gamma_{12}, \Gamma_{23}, \Gamma_{31}$ be meridian disks of $N(G)$ corresponding to edges b_{12}, b_{23}, b_{31} . Let $\gamma_{ij} = \partial \Gamma_{ij}$. See Figure 3.5.

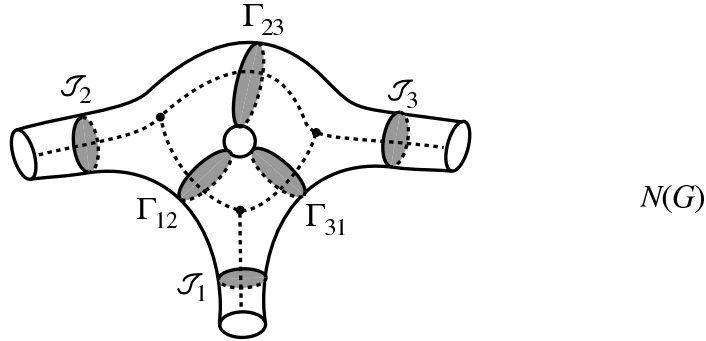


FIGURE 3.5

Definition 7. $X(G) = \text{exterior of } G = B^3 - (N(G) \cup N(\partial B^3))$. Note that $\partial X(G)$ is a surface of genus 3.

Definition 8. G is a *solution graph* iff it is a wagon wheel graph with the property that deleting any one of the edges $\{e_1, e_2, e_3\}$ from G gives a subgraph that is planar.

Definition 9. G is an *in trans solution graph* iff it is a wagon wheel graph with the property that deleting any one of the edges $\{e_1, e_2, e_3, b_{23}\}$ from G gives a subgraph that is planar.

The graphs G in Figure 3.6 are *in trans* solution graphs.

Definition 10. Let G be a wagon wheel graph. A 3-string tangle \mathcal{T} is *carried by* G , written $\mathcal{T}(G)$, iff its 3-strings s_{12}, s_{23}, s_{31} can be (simultaneously) isotoped to lie in $\partial N(G)$ such that

- 1) s_{ij} intersects each of J_i, J_j once
- 2) s_{ij} intersects γ_{ij} once and is disjoint from the remaining γ_{st} .

Figures 3.6 gives examples of tangles carried by wagon wheel graphs.

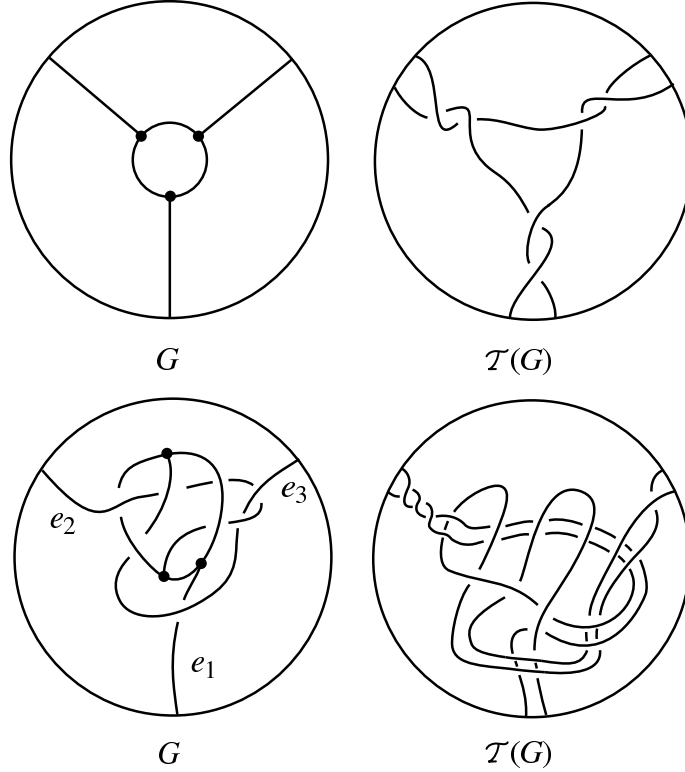


FIGURE 3.6

Lemma 3.3. *If T_1, T_2 are both carried by G , then they are isotopic in B^3 (rel endpoints) up to twisting $N(G)$ along the J_i (i.e., they differ by twists at the ends).*

Proof. Left to the reader. □

Lemma 3.4. *If a 3-string tangle T is carried by a planar wagon wheel graph G then T is standard.*

Proof. There is an isotopy of B^3 , keeping the boundary of B^3 fixed, taking G to the planar wagon wheel graph of Figure 3.6 (upper left). Apply Lemma 3.3 to see T as standard. □

The following theorem and corollary lets us work with graphs rather than tangles. The solution graph economically encodes the conditions needed for a solution tangle.

Theorem 3.5. *Let \mathcal{T} be a solution tangle, then \mathcal{T} is carried by a solution graph. Conversely, a solution graph carries a unique solution tangle.*

Proof. Let \mathcal{T} be a solution tangle with strands s_{12}, s_{23}, s_{31} . We show that \mathcal{T} is carried by a solution graph G . Let $C = c_1 \cup s_{12} \cup c_2 \cup s_{23} \cup c_3 \cup s_{31}$, recalling that the c_i are the capping arcs of Figure 2.13. For each $i = 1, 2, 3$, let P_i be a point in c_i . Isotope C into the interior of B^3 by pushing each c_i slightly to the interior. Under the isotopy P_i traces out an arc e_i from $P_i \in \partial B_3$ to C .

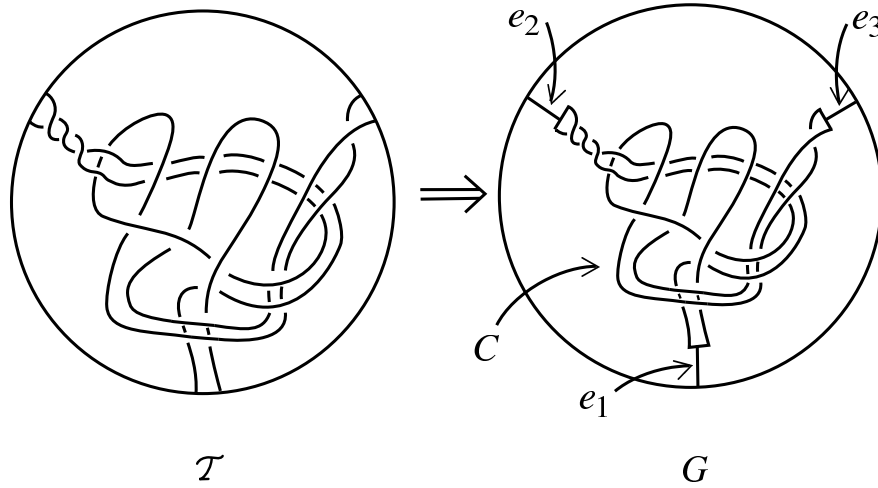


FIGURE 3.7

Define $G = C \cup e_1 \cup e_2 \cup e_3$. See Figure 3.7. G is a wagon wheel graph that carries \mathcal{T} . Note that the strings s_{ij} of \mathcal{T} correspond to the edges b_{ij} of G . The conditions for \mathcal{T} to be a solution tangle now correspond to those defining G as a solution graph. For example, if \mathcal{T} is a solution tangle, $s_{23} \cup (s_{12} \cup c_1 \cup s_{31}) \cup c_2 \cup c_3$ (where c_1 has been pushed into the interior of B^3) lies in a properly embedded disk D in B^3 . Hence $G - e_1$ lies in D and is planar.

We now show that a solution graph carries a unique solution tangle. By Lemma 3.3 the tangles carried by G are parameterized by integers n_1, n_2, n_3 as in Figure 3.8 (where the boxes are twist boxes). Denote these tangles by $\mathcal{T}(n_1, n_2, n_3)$. As G is a solution graph, $\mathcal{T}(0, 0, 0) \cup c_i$ will be the 2-string tangle $\frac{1}{f_i}$, where $f_i \in \mathbb{Z}$. Then $\mathcal{T}(n_1, n_2, n_3) \cup c_i$

will be the 2-string tangle $\frac{1}{f_i+n_j+n_k}$ where $\{i, j, k\} = \{1, 2, 3\}$.

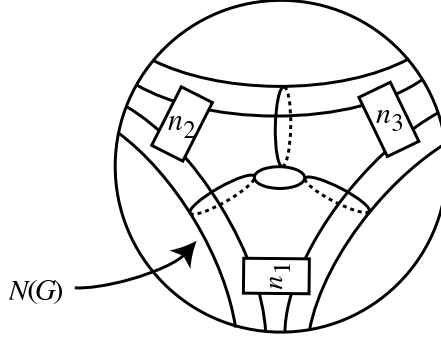


FIGURE 3.8

Based on Lemma 2.1, we choose n_i, n_j, n_k to satisfy

$$n_1 + n_2 + f_3 = -4$$

$$n_2 + n_3 + f_1 = -4$$

$$n_3 + n_1 + f_2 = -4$$

Since $f_1 + f_2 + f_3$ is even, this has a unique integer solution. Then $\mathcal{T}(n_1, n_2, n_3) \cup c_i = \frac{1}{-4}$ tangle for each i . Thus \mathcal{T} is a solution tangle.

The uniqueness of \mathcal{T} follows from the parameterization of the tangles by the n_i and the fact that $\mathcal{T} \cup c_i = \frac{1}{-4}$ tangle.

□

Corollary 3.6. *Let \mathcal{T} be an in trans solution tangle, then \mathcal{T} is carried by an in trans solution graph. Conversely, an in trans solution graph carries a unique in trans solution tangle.*

Proof. Let \mathcal{T} be an in trans solution tangle. Since \mathcal{T} is an in trans solution tangle, \mathcal{T} is a solution tangle. Hence \mathcal{T} is carried by a solution graph, G . $G - b_{23}$ corresponds to the graph $s_{12} \cup c_1 \cup s_{31} \cup e_1$. As \mathcal{T} is an in trans solution tangle, $s_{12} \cup c_1 \cup s_{31}$ lies in a properly embedded disk D in B^3 . Hence $G - b_{23}$ lies in D and is planar. Thus G is an in trans solution graph.

Suppose G is an in trans solution graph. Thus G is a solution graph and carries a solution tangle. Since G is an in trans solution graph, $G - b_{23}$ is also planar. Then the 2-string tangle $\mathcal{T}(n_1, n_2, n_3) - s_{23} = \frac{1}{f}$ for some integer f . Furthermore, we have chosen n_1, n_2, n_3 so that $\ell k(x_{ij} \cup s_{ij}, \hat{s}_i \cup \hat{x}_i) = -2$. The argument of Lemma 2.2 shows that $\ell k(x_{12} \cup s_{12}, x_{31} \cup s_{31}) = -1$. Thus $\mathcal{T}(n_1, n_2, n_3) - s_{23} = \frac{1}{-2}$ tangle. Therefore \mathcal{T} is an in trans solution tangle. \mathcal{T} is unique by Theorem 3.5.

□

Corollary 3.6 allows us to construct infinitely many *in trans* solution tangles, via *in trans* solution graphs. Recall that a *Brunnian link*, L , is one such that once any component is removed the remaining components form the unlink. By piping a Brunnian link to a given *in trans* solution graph, we generate a new *in trans* solution graph as pictured in Figure 3.9 (where we have begun with the second solution graph of Figure 3.6). Similar results hold for solution tangles.

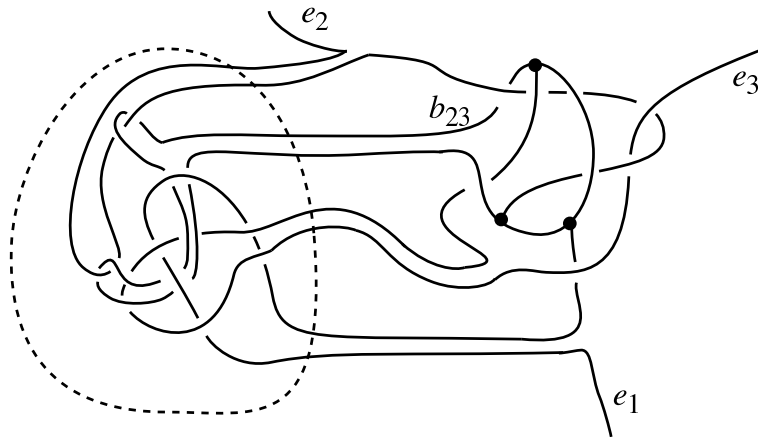


FIGURE 3.9

3.2. Wagon wheel graphs and tetrahedral graphs. Attaching a 3-ball, B' , to the 3-ball B^3 in which G lies, then collapsing B' to a point, gives a new graph, \widehat{G} , in the 3-sphere. \widehat{G} is a tetrahedral graph in S^3 , i.e. a graph abstractly homeomorphic to the 1-skeleton of a tetrahedron. The edges of \widehat{G} are those of G : $e_1, e_2, e_3, b_{12}, b_{23}, b_{31}$. The planarity of G (i.e. lying on a disk in B^3) then corresponds to the planarity of \widehat{G} in S^3 (i.e. lying on a 2-sphere in S^3). Also, the exteriors of G and \widehat{G} , in B^3 and S^3 (resp.), are homeomorphic.

Definition 11. A surface F in a 3-manifold M is *compressible* if there is a disk D embedded in M such that $D \cap F = \partial D$ and ∂D does not bound a disk in F . F is *incompressible* otherwise (where F is not a 2-sphere).

Recall a graph is abstractly planar in S^3 if there exists an embedding of it onto a 2-sphere in S^3 . We are now in a position to use the following characterization of planar graphs in the 3-sphere.

Theorem 3.7. (Theorem 2.0 of [T], see also [ST]) Let \widehat{G} be an abstractly planar graph embedded in S^3 . \widehat{G} is planar if and only if:

- (1) Every proper subgraph of \widehat{G} is planar, and
- (2) $X(\widehat{G}) = S^3 - \text{int}(N(\widehat{G}))$ has compressible boundary.

Lemma 3.8. Let e_n , $n = 1, 2, 3$, be three edges of the tetrahedral graph \widehat{G} which share a common vertex and suppose $\widehat{G} - e_n$ is planar for $n = 1, 2, 3$. Suppose there is a fourth edge, b_{jk} , such that $X(\widehat{G} - b_{jk})$ has compressible boundary. Then $\widehat{G} - b_{jk}$ is a planar graph in S^3 .

Proof. We can think of $\widehat{G} - b_{jk}$ as a theta-curve graph, $\widehat{\Theta}$, with two vertices and three edges e_i , $e_j \cup b_{ij}$, and $e_k \cup b_{ki}$. Since $\widehat{G} - e_n$ is planar for $n = 1, 2, 3$, the subgraphs $(\widehat{G} - b_{jk}) - e_i$, $(\widehat{G} - b_{jk}) - (e_j \cup b_{ij})$, and $(\widehat{G} - b_{jk}) - (e_k \cup b_{ki})$ are all planar subgraphs. Since $X(\widehat{G} - b_{jk})$ has compressible boundary, $\widehat{G} - b_{jk}$ is a planar graph in S^3 by Theorem 3.7. \square

A tetrahedral graph, its corresponding wagon wheel graph, and the tangles carried by the wagon wheel graph are all related by their exterior.

Definition 12. Let \mathcal{T} be a 3-string tangle with strings s_{12}, s_{23}, s_{31} . $X(\mathcal{T}) = B^3 - \text{nbhd}(s_{12} \cup s_{23} \cup s_{31} \cup \partial B^3)$.

Lemma 3.9. If \mathcal{T} is carried by the wagon wheel graph G and if \widehat{G} is the corresponding tetrahedral graph, then $X(G) = X(\widehat{G})$ is isotopic to $X(\mathcal{T})$ and $X(G - b_{ij}) = X(\widehat{G} - b_{ij})$ is isotopic to $X(\mathcal{T} - s_{ij})$.

Proof. See Figure 3.7. \square

3.3. Rational tangles. \mathcal{T} is *rational* if there is an isotopy of B^3 taking \mathcal{T} to a tangle containing no crossings. Rational tangle solutions are generally believed to be the most likely biological models. For simplification we model a protein-DNA complex as a 3-ball (the protein) with properly embedded strings (the DNA segments). However, it is believed in many cases that the DNA winds around the protein surface without crossing itself. Thus, if we push the DNA inside the ball, we have a rational tangle.

Lemma 3.10. Suppose a rational tangle \mathcal{T} is carried by G , then $X(G)$ has compressible boundary and $X(G - b_{jk})$ has compressible boundary for all b_{jk} .

Proof. If \mathcal{T} is rational, then there is a disk, D , separating s_{ij} from s_{ik} . Thus $X(G)$ has compressible boundary. This disk D also separates the two strands of $\mathcal{T} - s_{jk}$ and thus $X(\mathcal{T} - s_{jk})$ has compressible boundary. Since $X(\mathcal{T} - s_{jk})$ and $X(G - b_{jk})$ are homeomorphic, $X(G - b_{jk})$ has compressible boundary. \square

Corollary 3.11. *Suppose \mathcal{T} is rational and \mathcal{T} is a solution tangle, then \mathcal{T} is the PJH tangle.*

Proof. By Theorem 3.5, \mathcal{T} is carried by a solution graph G . Thus, $G - e_n$ is planar for $n = 1, 2, 3$. By Lemma 3.10, $X(G)$ has compressible boundary and $X(G - b_{jk})$ has compressible boundary for all b_{jk} . Lemmas 3.9 and 3.8 imply $\widehat{G} - b_{jk}$ (where \widehat{G} is the tetrahedral graph corresponding to G) is planar for all b_{jk} , and hence \widehat{G} is planar (Theorem 3.7). Thus G is planar. By Lemma 3.4, \mathcal{T} is standard and hence the PJH tangle (Lemma 3.1). \square

Proposition 2.5 allows us to extend the results of this section to experiments in which the *in cis* deletion products are $(2, p)$ torus links (rather than specifically $(2, 4)$). For example, the analog of Corollary 3.11 would state that if the synaptic tangle is rational, then three $(2, p)$ torus link *in cis* products would force it to be standard (plectonemic form) as in Figure 3.1.

In contrast to Corollary 3.11, the examples in Figures 3.10 and 3.11, as discussed in the proof of Theorem 3.12, show that no other set of three deletion experiments would be enough to determine that a solution \mathcal{T} is standard just from the knowledge that it is rational.

Theorem 3.12. *A system of four deletion experiments with $(2, p)$ torus link products must include all three *in cis* experiments to conclude that a rational tangle satisfying this system is standard.*

Proof. For the tetrahedral graph in Figure 3.10, $\widehat{G} - e_1$, $\widehat{G} - b_{12}$, $\widehat{G} - b_{31}$, $\widehat{G} - b_{23}$ are all planar subgraphs. Deleting a neighborhood of the vertex adjacent to the e_i 's results in a wagonwheel graph, G . The subgraph $G - e_2$ carries a 2-string tangle which is not rational. Hence $G - e_2$ is not planar and thus G is not planar, yet it does carry a rational tangle. Thus three *in trans* experiments and one *in cis* experiments is not sufficient to determine \mathcal{T} is standard under the assumption that \mathcal{T} is rational.

Instead of removing a neighborhood of the vertex adjacent to the e_i 's, we can delete a neighborhood of the vertex adjacent to the edges e_2 , b_{12} , and b_{23} from the tetrahedral

graph in Figure 3.10. In this case, we also obtain a wagon wheel graph carrying a rational tangle which is not standard. Hence the nonplanar tetrahedral graph in Figure 3.10 can also be used to show that two *in trans* and two *in cis* experiments, where three of the four corresponding edges in the tetrahedral graph share a vertex, is also not sufficient to determine \mathcal{T} is standard.

The tetrahedral graph in Figure 3.11 is not planar as $\widehat{G} - e_2 - b_{31}$ is knotted. However, $\widehat{G} - e_1$, $\widehat{G} - e_3$, $\widehat{G} - b_{23}$, and $\widehat{G} - b_{12}$ are all planar. Hence this graph shows that the remaining case, two *in trans* and two *in cis* experiments where no three of the four corresponding edges in the tetrahedral graph share a common vertex, is also not sufficient to determine \mathcal{T} is standard.

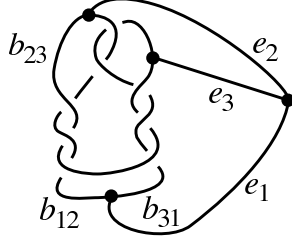


FIGURE 3.10

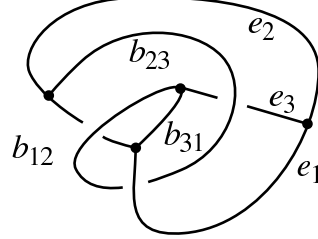


FIGURE 3.11

□

3.4. The exterior $X(G)$. Our goal is to prove Corollary 3.20, which extends Corollary 3.11. In Section 4, we will use Corollary 3.20 to show there is a unique small crossing solution tangle. We first establish some properties of the exterior of both solution graphs and *in trans* solution graphs.

Definition 13. Let M be a 3-manifold, F a subsurface of ∂M , and J a simple closed curve in F . Then $\tau(M, J)$ is the 3-manifold obtained by attaching a 2-handle to M along J . That is, $\tau(M, J) = M \cup_J H$, where H is a 2-handle. $\sigma(F, J)$ is the subsurface of $\partial\tau(M, J)$ obtained by surgering F along ∂H . That is, $\sigma(F, J) = (F \cup \partial H) - \text{int}(F \cap \partial H)$.

Handle Addition Lemma. ([J],[CG],[Sch], [Wu1]) *Let M be an orientable, irreducible 3-manifold and F a surface in ∂M . Let J be a simple, closed curve in F . Assume $\sigma(F, J)$ is not a 2-sphere. If F is compressible in M but $F - J$ is incompressible, then $\sigma(F, J)$ is incompressible in $\tau(M, J)$.*

Lemma 3.13. *Let G be a wagon wheel graph and $X(G)$ its exterior. Let J_i and γ_{ij} be the meridian curves on $\partial X(G)$ in Figure 3.5 (and defined right above the figure). Suppose*

$\partial X(G)$ compresses in $X(G)$. If G is a solution graph, then $\partial X(G) - (J_1 \cup J_2 \cup J_3)$ is compressible in $X(G)$. If G is an *in trans* solution graph, then $\partial X(G) - (\gamma_{23} \cup J_1 \cup J_2 \cup J_3)$ is compressible in $X(G)$.

Proof. Assume $\partial X(G)$ compresses in $X(G)$. Note that $X(G)$ is irreducible. We will use the following four claims to prove this lemma:

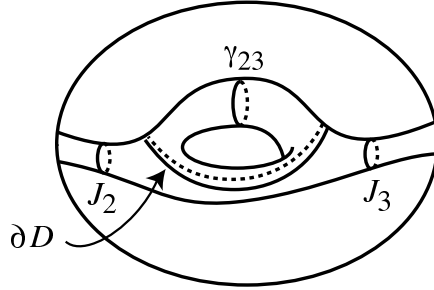
Claim 3.14. *If $G - b_{23}$ is planar (e.g., G is an *in trans* solution graph), then $\partial X(G) - \gamma_{23}$ is compressible in $X(G)$.*

Proof. Since $G - b_{23}$ is planar, $\tau(X(G), \gamma_{23}) = X(G - b_{23})$ has compressible boundary. The claim now follows from the Handle Addition Lemma. \square

If G is an *in trans* solution graph, let $F_1 = \partial X(G) - \gamma_{23}$. By Claim 3.14, F_1 is compressible in $X(G)$. Else if G is a solution graph, let $F_1 = \partial X(G)$. In this case, F_1 is compressible in $X(G)$ by hypothesis.

Claim 3.15. *$F_2 = F_1 - J_1$ is compressible in $X(G)$.*

Proof. F_1 is compressible in $X(G)$. On the other hand, since $\tau(X(G), J_1) = X(G - e_1)$ and $G - e_1$ is planar, $\sigma(F_1, J_1)$ compresses in $\tau(X(G), J_1)$, see Figure 3.12. The claim now follows from the Handle Addition Lemma. \square



$D = \text{compressing disk}$

FIGURE 3.12

Claim 3.16. *$F_3 = F_2 - J_2$ is compressible in $X(G)$.*

Proof. Since $G - e_2$ is planar, $\sigma(F_2, J_2)$ is compressible in $\tau(X(G), J_2)$ (as in the analog of Figure 3.12). Thus Claim 3.15 with the Handle Addition Lemma implies the claim. \square

Claim 3.17. *$F = F_3 - J_3$ is compressible in $X(G)$.*

Proof. $G - e_3$ is planar, hence $\sigma(F_3, J_3)$ is compressible in $\tau(X(G), J_3) = X(G - e_3)$ (as in the analog of Figure 3.12). Claim 3.16 with the Handle Addition Lemma says that $F_3 - J_3$ is compressible in $X(G)$. \square

Thus if G is a solution graph, then $F = \partial X(G) - (J_1 \cup J_2 \cup J_3)$ is compressible in $X(G)$. If G is an *in trans* solution graph, then $F = \partial X(G) - (\gamma_{23} \cup J_1 \cup J_2 \cup J_3)$ is compressible in $X(G)$. \square (Lemma 3.13)

3.5. Solution graphs.

Lemma 3.18. *Let G be a solution graph and $X(G)$ its exterior. Let J_i and γ_{ij} be the meridian curves on $\partial X(G)$ in Figure 3.5 (and defined right above the figure). If $\partial X(G)$ compresses in $X(G)$, then there is a properly embedded disk in $X(G)$ that intersects each γ_{ij} algebraically once in $\partial X(G)$ and is disjoint from the J_i .*

Proof. Let D' be a disk, guaranteed by Lemma 3.13, properly embedded in $X(G)$ such that $\partial D' \subset F = \partial X(G) - (J_1 \cup J_2 \cup J_3)$ and $\partial D'$ does not bound a disk in F . Write $B^3 = X(G) \cup_{\partial X(G)} M$ where $M = \text{nbhd}(G \cup \partial B^3)$. In the notation of Figure 3.5, let $M - \text{nbhd}(\mathcal{J}_1 \cup \mathcal{J}_2 \cup \mathcal{J}_3) = M_1 \cup M_2$ where M_1 is $S^2 \times I$ and M_2 is a solid torus. If $\partial D'$ lies in ∂M_1 , we can form a 2-sphere, S , by capping off D' with a disk in M_1 (take the disk bounded by $\partial D'$ on ∂M_1 and push in slightly). That is, S is a 2-sphere which intersects $\partial X(G)$ in $\partial D'$. But then S would have to be non-separating (there would be an arc from \mathcal{J}_1 to \mathcal{J}_2 , say, on ∂M_1 which intersected $\partial D'$ once and an arc connecting \mathcal{J}_1 to \mathcal{J}_2 on ∂M_2 which missed $\partial D'$, hence S , altogether). But 2-spheres in a 3-ball are separating.

Thus $\partial D'$ must lie in ∂M_2 . If $\partial D'$ is essential in ∂M_2 , then $\partial D'$ must intersect any meridian of the solid torus M_2 algebraically once (else B^3 would contain a lens space summand). Then D' is the desired disk, and we are done. So assume $\partial D'$ bounds a disk, D'' , in ∂M_2 . Then the disks $\text{nbhd}(\mathcal{J}_1 \cup \mathcal{J}_2 \cup \mathcal{J}_3) \cap \partial M_2$ must lie in D'' , as $S = D' \cup D''$ is separating. Since $G - e_1$ is planar, M_2 is an unknotted solid torus in B^3 . Thus there is a properly embedded disk $D \subset B^3 - \text{int} M_2$ such that ∂D is a longitude of ∂M_2 and hence is essential. Furthermore, we can arrange that D is disjoint from D'' . Then $D \cap S$ is a collection of trivial circles in D' and D can be surgered off S without changing ∂D . In particular, D is properly embedded in $X(G)$ since the e_i lie on the opposite side of S from D . D is the desired disk. \square

Definition 14. Let \mathcal{T} be a 3-string tangle. \mathcal{T} is *split* if there is a properly embedded disk separating two of its strands from the third (Figure 3.13(a)). Strands s_1, s_2 of \mathcal{T} are *parallel* if there is a disk D in B^3 such that $\text{int}(D)$ is disjoint from \mathcal{T} and $\partial D = s_1 \cup \alpha \cup s_2 \cup \beta$ where α, β are arcs in ∂B^3 (Figure 3.13(b)).

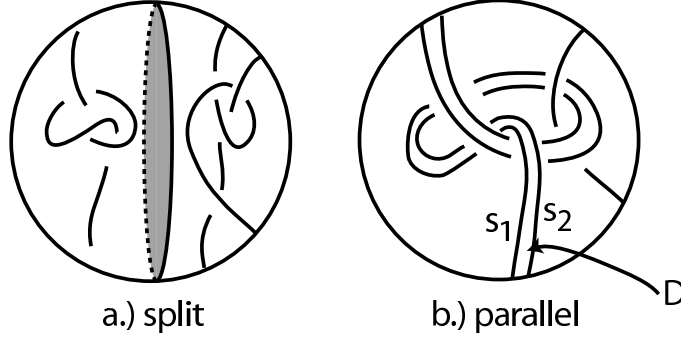


FIGURE 3.13

Note: Rational tangles are split and have parallel strands.

Lemma 3.19. *Let \mathcal{T} be a 3-string tangle carried by a solution graph G . If \mathcal{T} is rational, split, or if \mathcal{T} has parallel strands, then $X(G)$ and $X(G - b_{ij})$, for each i, j , have compressible boundary.*

Proof. If \mathcal{T} is rational, split, or has parallel strands then $\partial X(\mathcal{T})$ is compressible in $X(\mathcal{T})$. By Lemma 3.9, $\partial X(G)$ is compressible in $X(G)$.

We now argue that $\partial X(G - b_{ij})$ is compressible in $X(G - b_{ij})$. Below $\{i, j, k\} = \{1, 2, 3\}$.

If \mathcal{T} is split, then there is a disk, D , separating one strand from two. If s_{ij} is on the side of D containing two, then D still separates the two strands of $\mathcal{T} - s_{ij}$ and $X(\mathcal{T} - s_{ij})$ still has compressible boundary. By Lemma 3.9, $X(G - b_{ij})$ has compressible boundary. So we assume s_{ij} is on one side of D and s_{jk}, s_{ki} on the other. As a disk properly embedded in $X(G)$, D separates the curves γ_{ij}, γ_{jk} of $\partial X(G)$. By Lemma 3.18 there is a disk D' in $X(G)$ that intersects γ_{jk} on $\partial X(G)$ algebraically a non-zero number of times. After surgering along D (while preserving the non-zero algebraic intersection with γ_{jk}), we may assume that D' is disjoint from D , and hence from γ_{ij} . But then D' is a compressing disk for $G - b_{ij}$.

If \mathcal{T} has parallel strands, we argue in two cases according to which strands are parallel:

First, assume s_{jk}, s_{ki} are parallel. Then they are parallel in $\mathcal{T} - s_{ij}$ and $X(\mathcal{T} - s_{ij})$ has compressible boundary. By Lemma 3.9 then $X(G - b_{ij})$ has compressible boundary.

So, assume that s_{ij} and s_{jk} are parallel. Then there is a disk, D , properly embedded in $X(G)$ that intersects γ_{ij} exactly once, γ_{jk} exactly once, and is disjoint from γ_{ki} . By

Lemma 3.18, there is also a disk, D' , in $X(G)$ that intersects γ_{ki} algebraically once. After possibly surgering D' along D we may assume the D and D' are disjoint. But $X(G - nbhd(D))$ is homeomorphic to $X(G - b_{ij})$, and D' becomes a compressing disk in $X(G - b_{ij})$. □

Corollary 3.20. *Let \mathcal{T} be a solution tangle. If \mathcal{T} is rational or split or if \mathcal{T} has parallel strands, then \mathcal{T} is the PJH tangle.*

Proof. Let G be a solution graph carrying \mathcal{T} . Then Lemmas 3.19, 3.9 and 3.8 imply that $\widehat{G} - b_{jk}$ planar for all b_{jk} where \widehat{G} is the associated tetrahedral graph. Thus Theorem 3.7 implies \widehat{G} is planar. Thus G is planar. By Lemma 3.4, \mathcal{T} is standard. Now Lemma 3.1 says \mathcal{T} is the PJH tangle. □

Remark. Since *in trans* solution tangles are also solution tangles, Corollary 3.20 also applies to *in trans* solution tangles. Although the three *in cis* deletion equations suffice to determine \mathcal{T} if \mathcal{T} is rational, split or has parallel strands, the *in trans* deletion experiment does rule out some exotic solutions. For example, the tangle in Figure 3.14 satisfies all the *in cis* experimental results (*i.e.* it is a solution tangle), but does not satisfy the *in trans* results (*i.e.* it is not an *in trans* solution tangle).

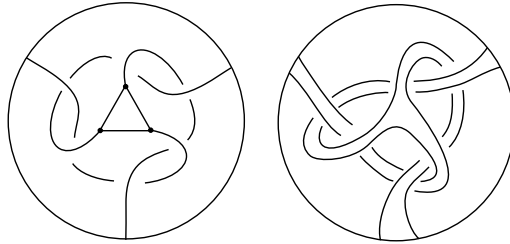


FIGURE 3.14

3.6. *In trans* solution graphs. In Lemma 3.21 we will show that the exterior of an *in trans* solution graph is a handlebody. This need not be true for solution graphs. The solution graph of Figure 3.14 contains an incompressible genus 2 surface in its exterior (it is based on Thurston's *trapos* graph). Thus its exterior is not a handlebody. We will also use Lemma 3.21 to further explore planarity of tetrahedral graphs in the next section.

Lemma 3.21. *Let G be an *in trans* solution graph and $X(G)$ its exterior. Let J_i and γ_{ij} be the meridian curves on $\partial X(G)$ in Figure 3.5 (and defined right above the figure). If $\partial X(G)$ compresses in $X(G)$, then there is a properly embedded disk in $X(G)$ that*

intersects γ_{23} exactly once, intersects each of γ_{12}, γ_{31} algebraically once, and is disjoint from the J_i . Furthermore, $X(G)$ is a handlebody.

Proof. By Lemma 3.13, there is a disk D' properly embedded in $X(G)$ such that $\partial D' \subset F = \partial X(G) - (\gamma_{23} \cup J_1 \cup J_2 \cup J_3)$ and $\partial D'$ does not bound a disk in F . Write $B^3 = X(G) \cup_{\partial X(G)} M$ where $M = nbhd(G \cup \partial B^3)$. In the notation of Figure 3.5, let $M - nbhd(\mathcal{J}_1 \cup \mathcal{J}_2 \cup \mathcal{J}_3 \cup \Gamma_{23}) = M_1 \cup M_2$ where M_1 is $S^2 \times I$ and M_2 is a 3-ball. $\partial D'$ lies in ∂M_i for some i , hence we can form a 2-sphere, S , by capping off D' with a disk in M_i (take the disk bounded by $\partial D'$ on ∂M_i and push in slightly). That is, S is a 2-sphere which intersects $\partial X(G)$ in $\partial D'$. If $\partial D'$ lay on ∂M_1 , then S would have to be non-separating (there would be an arc from \mathcal{J}_1 to \mathcal{J}_2 , say, on ∂M_1 which intersected $\partial D'$ once and an arc connecting \mathcal{J}_1 to \mathcal{J}_2 on ∂M_2 which missed $\partial D'$, hence S , altogether). But 2-spheres in a 3-ball are separating.

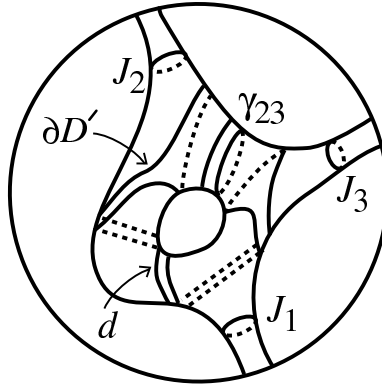


FIGURE 3.15

Thus $\partial D'$ must lie in ∂M_2 . But then in ∂M_2 , the disks $nbhd(\mathcal{J}_1 \cup \mathcal{J}_2 \cup \mathcal{J}_3) \cap \partial M_2$ must lie on opposite sides of $\partial D'$ from the disks $\Gamma'_{23} \cup \Gamma''_{23} = nbhd(\Gamma_{23}) \cap \partial M_2$, as S is separating. Thus S can be isotoped to intersect $N(G)$ in the curve gotten by connecting the two disks $\Gamma'_{23}, \Gamma''_{23}$ by a band d lying in $\partial N(G)$. See Figure 3.15. We may view S as a 2-sphere which intersects G in only two points and separates off a subarc b'_{23} of b_{23} . Now b'_{23} must be unknotted in the 3-ball bounded by S , otherwise deleting e_1 would not give a planar graph. Hence, there exists a disk D in the 3-ball bounded by S such that the boundary of D consists of the arc b'_{23} and an arc in $\Gamma'_{23} \cup \Gamma''_{23} \cup d$. Then D can be taken to be a disk, properly embedded in $X(G)$ whose boundary is disjoint from $J_1 \cup J_2 \cup J_3$ and whose boundary intersects γ_{23} exactly once. Finally, as γ_{12}, γ_{31} are isotopic to γ_{23} on the boundary of the solid torus component of $M - nbhd(\mathcal{J}_1 \cup \mathcal{J}_2 \cup \mathcal{J}_3)$, ∂D intersects

these curves algebraically once. Furthermore, $X(G \cup D)$ is homeomorphic to $X(G - \gamma_{23})$, which is a handlebody. Thus $X(G)$ is a handlebody. \square

3.7. Tetrahedral graph planarity. In the above model, each mathematical assumption about the planarity of the *in trans* solution graph after deleting an edge corresponds to an experimental result. For the economy of experiment, then, it is natural to ask how much information is necessary to conclude the planarity of the graph. Recall that by collapsing the outside 2-sphere to a vertex, a wagon wheel graph in B^3 becomes a tetrahedral graph \widehat{G} in S^3 . We discuss this issue of economy in the context of tetrahedral graphs and in the spirit of Theorem 3.7 (see also [ST], [Wu2], [G]). In particular, Theorem 3.22 and Corollary 3.25 say that, in contrast to Theorem 3.7, to check the planarity of a tetrahedral graph, one does not need to check the planarity of *all* subgraphs. We end with examples showing that Corollary 3.25 is sharp.

Theorem 3.22. *Let \widehat{G} be a tetrahedral graph. Then \widehat{G} is planar if and only if*

- (1) *the exterior of \widehat{G} has compressible boundary; and*
- (2) *there is an edge, ϵ' , of \widehat{G} such that for any edge $e \neq \epsilon'$ of \widehat{G} , $\widehat{G} - e$ is planar.*

Proof. If \widehat{G} is planar then clearly the two conditions hold. We prove the converse: the two listed conditions on \widehat{G} guarantee that \widehat{G} is planar. Let ϵ be the edge of \widehat{G} which does not share an endpoint with ϵ' .

Let e_1, e_2, e_3, e_4 be the four edges of \widehat{G} other than ϵ, ϵ' . Let d_i be the meridian disk corresponding to the edge e_i in $\text{nbhd}(\widehat{G})$ and let $m_i = \partial d_i$ be the corresponding meridian curve on the boundary of $X(\widehat{G})$, the exterior of \widehat{G} .

Claim 3.23. *$X(\widehat{G})$ is a handlebody.*

Proof. Pick a vertex, v , of \widehat{G} not incident to ϵ' . Then removing a neighborhood of v from S^3 , \widehat{G} becomes an *in trans* solution graph G in a 3-ball. Furthermore, $X(G)$ is homeomorphic to $X(\widehat{G})$. The Claim now follows from Lemma 3.21. \square

Recall the following from [G].

Theorem 3.24. *Let \mathcal{C} be a set of $n + 1$ disjoint simple loops in the boundary of a handlebody X of genus n , such that $\tau(X; \mathcal{C}')$ is a handlebody for all proper subsets \mathcal{C}' of \mathcal{C} . Then $\cup \mathcal{C}$ bounds a planar surface P in ∂X such that $(X, P) \cong (P \times I, P \times 0)$, where $I = [0, 1]$.*

Set $X = X(\widehat{G})$ and $\mathcal{C} = \{m_1, m_2, m_3, m_4\}$. Since $\widehat{G} - e_i$ is planar for $i = 1, \dots, 4$, Theorem 3.24 implies that there is a planar surface P in $X(\widehat{G})$ whose boundary is $\{m_1, m_2, m_3, m_4\}$ and such that $(X(\widehat{G}), P) \cong (P \times I, P \times 0)$. Capping $P \times \frac{1}{2}$ with the meridian disks $\{d_1, d_2, d_3, d_4\}$ gives a 2-sphere \widehat{P} in S^3 disjoint from \widehat{G} except for a single point intersection with each of the edges e_1, e_2, e_3, e_4 . Let $\widehat{G} - \widehat{P} = G_1 \cup G_2$. Labeling the edges as in \widehat{G} , we take G_1 with edges $\{\epsilon, e_1, e_2, e_3, e_4\}$ and G_2 with edges $\{\epsilon', e_1, e_2, e_3, e_4\}$. Furthermore, we may label so that e_1, e_2 share a vertex in G_1 and e_2, e_4 share a vertex in G_2 . See Figure 3.16.

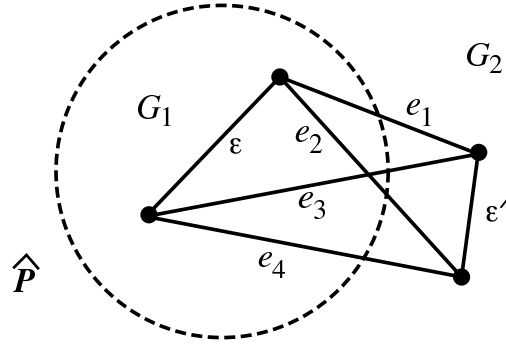


FIGURE 3.16

Let $N_1 = nbhd(G_1)$ and $N_2 = nbhd(G_2)$. Then $nbhd(\widehat{G})$ is the union of N_1 and N_2 along the meridian disks $\{d_1, d_2, d_3, d_4\}$. Now the pair $(N_i, \cup d_j) = (F_i \times I, \cup \alpha_i^j \times I)$ where $i \in \{1, 2\}$, $j \in \{1, 2, 3, 4\}$ and where each F_i is a disk, each α_i^j is an arc in ∂F_i . Each G_2 can be taken to lie in $F_i \times \{1/2\}$. Write $S^3 = B_1 \cup_{\widehat{P}} B_2$ where the B_i are 3-balls. Because $(X(\widehat{G}), P) \cong (P \times I, P \times 0)$, we may extend $F_i \times \{1/2\}$ to a properly embedded disk F'_i in B_i containing G_2 . By a proper choice of the initial F_i we may assume that $F'_i - (\cup \alpha_i^j)$ is a union of four arcs β_i^j , labelled as in Figure 3.17.

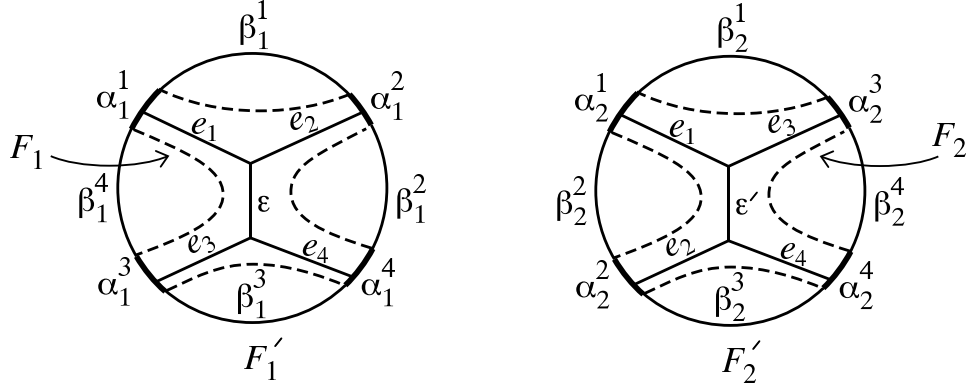


FIGURE 3.17

In particular,

- β_1^1 is isotopic to $e_1 \cup e_2$ and β_1^3 is isotopic to $e_3 \cup e_4$ in B_1 (keeping the endpoints in $\cup d_j$ on $\partial B_1 = \widehat{P}$).
- β_2^1 is isotopic to $e_1 \cup e_3$ and β_2^3 is isotopic to $e_2 \cup e_4$ in B_2 (keeping the endpoints in $\cup d_j$ on $\partial B_1 = \widehat{P}$).

The boundary of F'_1 frames the 4-punctured sphere $P \subset \widehat{P}$. This allows us to assign a rational number slope on properly embedded arcs in P (up to proper isotopy in P). We take β_1^1, β_1^3 to have slope $\frac{0}{1}$ and β_1^2, β_1^4 to have slope $\frac{1}{0}$. It follows that β_2^1, β_2^3 must have slope $\frac{1}{n}$: otherwise the edges e_1, e_2, e_3, e_4 of \widehat{G} will form a non-trivial 2-bridge knot, but we are assuming that $\widehat{G} - \epsilon$ is planar.

By re-choosing F_1 we may assume that β_1^2 is β_2^3 and that β_1^4 is β_2^1 . Then re-choosing F_2 (by twisting along the disk disjoint from $\beta_2^1 \cup \beta_2^3$ in B_2), we may further take β_2^2 to be β_1^1 and β_2^4 to be β_1^3 . Then $F'_1 \cup F'_2$ is a 2-sphere in S^3 containing \widehat{G} (Alternatively, instead of rechoosing F_2 , after rechoosing F_1 so that $\beta_1^2 = \beta_2^3$ and $\beta_1^4 = \beta_2^1$, we can extend F_1 to a disk containing $\widehat{G} - \epsilon'$. Thus $\widehat{G} - \epsilon'$ is planar and \widehat{G} is planar by Theorem 3.7). \square (Theorem 3.22)

We will now use Theorem 3.22 to prove Corollary 3.25.

Corollary 3.25. *Suppose \widehat{G} is a tetrahedral graph with the following properties:*

- (1) *There exists three edges $\epsilon_1, \epsilon_2, \epsilon_3$ such that $\widehat{G} - \epsilon_i$ is planar.*
- (2) *The three edges $\epsilon_1, \epsilon_2, \epsilon_3$ share a common vertex.*
- (3) *There exists two additional edges, ϵ_4 and ϵ_5 such that $X(\widehat{G} - \epsilon_4)$ and $X(\widehat{G} - \epsilon_5)$ have compressible boundary.*

(4) $X(\widehat{G})$ has compressible boundary.

Then \widehat{G} is planar.

Proof. By Lemma 3.8, $\widehat{G} - e_4$ and $\widehat{G} - e_5$ are planar. Thus by Theorem 3.22, \widehat{G} is planar. \square

We finish this section with examples that show that if any single hypothesis of Corollary 3.25 is dropped then its conclusion, that \widehat{G} is planar, may not hold. The tetrahedral graph in Figure 3.11 is not planar as $\widehat{G} - e_2 - b_{31}$ is knotted. However, $\widehat{G} - e_1$, $\widehat{G} - e_3$, $\widehat{G} - b_{23}$, and $\widehat{G} - b_{12}$ are all planar. Furthermore, $X(\widehat{G})$ is a handlebody as the edge b_{23} can be isotoped onto a neighborhood of $\widehat{G} - b_{23}$. (Alternatively, we can determine that $X(\widehat{G})$ is a handlebody by removing the vertex adjacent to the e_n 's, creating a wagon wheel graph, G , which carries a rational tangle \mathcal{T} . Since $X(\widehat{G}) = X(G) = X(\mathcal{T})$ and \mathcal{T} is rational, $X(\widehat{G})$ is a handlebody.) Thus $X(\widehat{G})$ has compressible boundary. $X(\widehat{G} - b_{31})$, and $X(\widehat{G} - e_2)$ also have compressible boundary. Thus properties 1, 3, 4 in Corollary 3.25 hold, but property 2 does not hold.

In Figure 3.10, $\widehat{G} - e_1$, $\widehat{G} - b_{12}$, $\widehat{G} - b_{31}$, $\widehat{G} - b_{23}$ are all planar graphs. The edges e_1 , b_{12} , and b_{31} share a common vertex. Since $\widehat{G} - b_{23}$ is planar, $X(\widehat{G} - b_{23})$ has compressible boundary. Removing the vertex adjacent to the e_n 's in \widehat{G} results in a wagon wheel graph, G , which carries a rational tangle. By Lemma 3.9 $X(G)$ is a handlebody, and thus $X(\widehat{G})$ has compressible boundary. On the other hand, $G - e_2$, $G - e_3$ carry tangles which are non-trivial disk sums that do not have compressible boundary (by Lemma 3.3 of [Wu3]). By Lemma 3.9, neither $X(G - e_2)$ nor $X(G - e_3)$ have compressible boundary. Hence neither $X(\widehat{G} - e_2)$ nor $X(\widehat{G} - e_3)$ have compressible boundary. In particular, \widehat{G} is not planar. Thus the tetrahedral graph in Figure 3.10 satisfies properties 1, 2, 4 in Corollary 3.25, but only satisfies half of property 3 ($X(\widehat{G} - b_{23})$ has compressible boundary, but there does not exist a fifth such edge).

Note that the tangle, \mathcal{T} , in Figure 3.18 is carried by a nonplanar wagon wheel graph, G . If G were planar, then \mathcal{T} would be the PJH tangle by Lemmas 3.4 and 3.1. To see that \mathcal{T} is not the PJH tangle, cap off these tangles by arcs along the tangle circle that are complementary to the c_i (*i.e.* the x_{ij} of Figure 2.4) to form 3 component links. These two 3-component links are not isotopic. For example, they have different hyperbolic volumes as computed by SnapPea. Let \widehat{G} be the tetrahedral graph corresponding to G . Every subgraph of \widehat{G} is planar. Hence conditions 1, 2, 3 of Corollary 3.25 hold, but $X(\widehat{G})$ does not have compressible boundary (by Theorem 3.7).

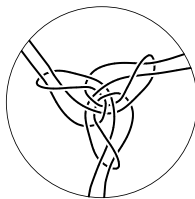


FIGURE 3.18

4. IF \mathcal{T} IS NOT THE PJH TANGLE, THEN $Cr(\mathcal{T}) \geq 8$ UP TO FREE ISOTOPY

Definition 15. Two 3-tangles $\mathcal{T}_1, \mathcal{T}_2$ are *freely isotopic* if there is an isotopy of the 3-ball, which is not necessarily fixed on its boundary, taking \mathcal{T}_1 to \mathcal{T}_2 .

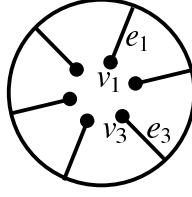
In the last section we showed that if a solution tangle is split or has two parallel strands, then it must be the PJH tangle. Here we show that if a tangle can be freely isotoped to have fewer than eight crossings, then it is either split or has two parallel strands. Hence a solution tangle which can be freely isotoped to have fewer than eight crossings must be the PJH tangle (Corollary 4.5). As a rational tangle is one which can be freely isotoped to have no crossings, one can think of Corollary 4.5 as a generalization of the result (Corollary 3.20) that the only rational solution tangle is the PJH tangle. Corollary 4.5 also gives a lower bound on the crossing number of an exotic solution tangle. Using the *in trans* deletion result, we will improve this lower bound in the next section after imposing a normal framing on the tangle (working with tangle equivalence rather than free isotopy).

Lemma 4.1. *If one string of a 3-tangle \mathcal{T} crosses the union of the other two strings at most once, then \mathcal{T} is split.*

Proof. If the string passes over the union, isotop the strand to the front hemisphere of the tangle sphere, otherwise isotop to the back. \square

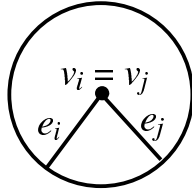
Definition 16. To a projection of a 3-string tangle \mathcal{T} we associate the 4-valent graph $\Gamma(\mathcal{T})$, that is obtained by placing a vertex at each crossing. If \mathcal{T} is not split, we label in sequence e_1, \dots, e_6 the distinct edges which are incident to the tangle circle. Let v_1, \dots, v_6

be the vertices of $\Gamma(\mathcal{T})$ which are endpoints of e_1, \dots, e_6 .



Lemma 4.2. *Assume \mathcal{T} is not split. If $v_i = v_j$ for some $i \neq j$, then the crossing number of its projection can be reduced by free isotopy.*

Proof. Assume $v_i = v_j$ with $i \neq j$. If e_i, e_j are opposing at v_i , then $e_i \cup e_j$ is a string of \mathcal{T} intersecting the other strings exactly once. By Lemma 4.1, \mathcal{T} is split. So we assume e_i, e_j are not opposing at v_i .



But then we can untwist e_i, e_j to reduce the crossing number. □

Definition 17. If \mathcal{T} is not split, let f_i be the face of $\Gamma(\mathcal{T})$ containing e_i, e_{i+1} .

Lemma 4.3. *Assume \mathcal{T} is not split. No two edges of f_i correspond to the same edge of $\Gamma(\mathcal{T})$. If two vertices of f_i correspond to the same vertex of $\Gamma(\mathcal{T})$, then the crossing number of the projection can be reduced by an isotopy fixed on the boundary. Finally, if v_j is incident to f_i , then $j \in \{i, i+1\}$ or a crossing can be reduced by a free isotopy.*

Proof. Assume that two edges of f_i correspond to the same edge of $\Gamma(\mathcal{T})$ (Figure 4.1). Then there would be a circle in the interior of the tangle circle intersecting the edge once. Then a string of \mathcal{T} intersects this circle exactly once contradicting the Jordan Curve Theorem.

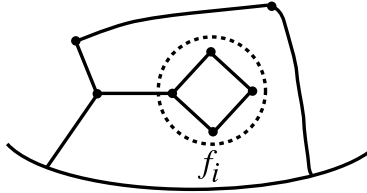


FIGURE 4.1

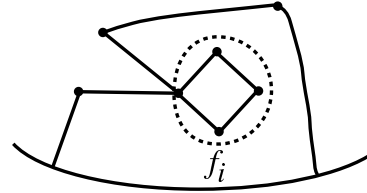


FIGURE 4.2

Similarly, if two vertices of f_i correspond to the same vertex, v , of $\Gamma(\mathcal{T})$, there would be a circle intersecting $\Gamma(\mathcal{T})$ only in v (Figure 4.2). This would give rise to a crossing that could be reduced by an isotopy rel ∂B^3 .

Now assume v_j is incident to f_i with $j \neq i, i+1$ (Figure 4.3). Then $e_j \notin f_i$ for otherwise \mathcal{T} would be split. Thus e_j lies in the exterior of f_i .

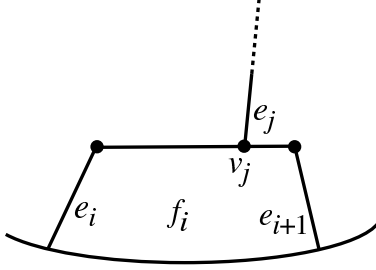


FIGURE 4.3

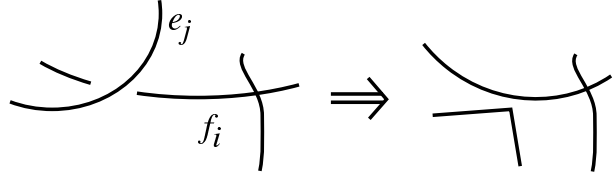


FIGURE 4.4

But now we can untwist the crossing at v_j by bringing e_j into f_i (Figure 4.4). □

Theorem 4.4. *If \mathcal{T} is a 3-string tangle which can be freely isotoped to a projection with at most seven crossings, then either \mathcal{T} is split or has two parallel strands.*

Proof. Note that \mathcal{T} being split or having parallel strands is invariant under free isotopy. Freely isotope \mathcal{T} to a minimal projection with ≤ 7 crossings and let $\Gamma(\mathcal{T})$ be the corresponding graph. Assume \mathcal{T} is not split. By Lemma 4.2, $\Gamma(\mathcal{T})$ has at least 6 vertices (thus \mathcal{T} has at least 6 crossings). If the six v_i are the only vertices incident to $\bigcup_i f_i$, then (Lemma 4.3) we must have Figure 4.5.

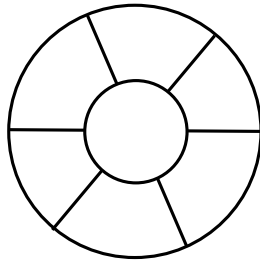


FIGURE 4.5

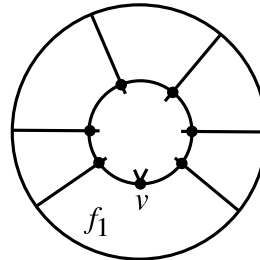


FIGURE 4.6

But then \mathcal{T} has a closed curve, a contradiction.

Thus $\Gamma(\mathcal{T})$ must have another vertex v lying on f_1 , say, which is not a v_i . Since \mathcal{T} has at most 7 crossings, there is exactly one such v and we have Figure 4.6. Enumerating the possibilities, we see there are nine cases, six of which are shown in Figure 4.7, while

the remaining three can be obtained from the top three via reflection:

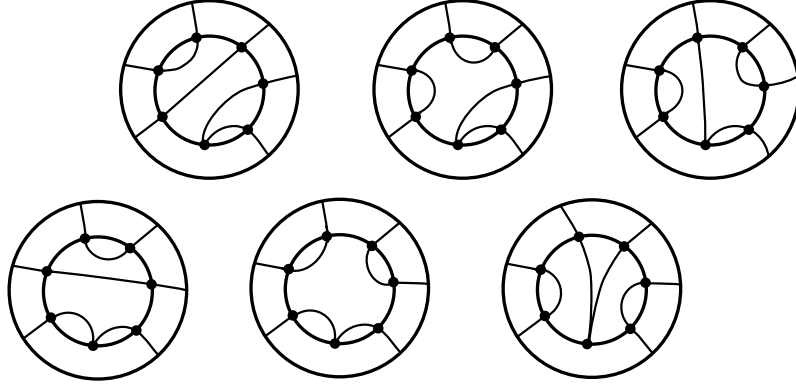


FIGURE 4.7

Note in each case we see two parallel strands (since we assumed \mathcal{T} is not split). For example, see Figure 4.8.

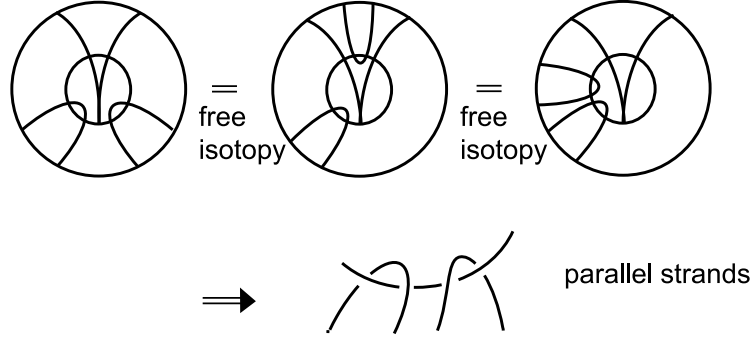


FIGURE 4.8

□

Theorem 4.4 and Corollary 3.20 imply the following:

Corollary 4.5. *Assume \mathcal{T} is a solution tangle. If \mathcal{T} can be freely isotoped to a projection with at most seven crossings, then \mathcal{T} is the PJH tangle.*

5. IF \mathcal{T} IS NOT THE PJH TANGLE, THEN \mathcal{T} HAS AT LEAST 10 CROSSINGS

Because the three DNA segments captured by the Mu transpososome in [PJH] are relatively short (50, 175 and 190 base pairs), one can argue that any projection of the transpososome must have few crossings. Let \mathcal{T} be an *in trans* solution tangle – a tangle satisfying both the *in cis* and the *in trans* deletion experiments. In this section we show that if \mathcal{T} is not the PJH tangle (Figure 2.4), then \mathcal{T} must be complicated, as measured by its minimal crossing number:

Proposition 5.1. *Let \mathcal{T} be an *in trans* solution tangle. If \mathcal{T} has a projection with fewer than 10 crossings, then \mathcal{T} is the PJH tangle.*

In this section, we are interested in crossing number up to tangle equivalence, that is, up to isotopy of the tangle fixed on the boundary. So we must fix a framing for our *in trans* solution tangle. We take that of Proposition 2.4, the normal form.

Remark. As pointed out in section 2, one goes from an *in trans* solution tangle in normal framing to one in the [PJH] framing by adding one left-handed twist at c_2 . Thus, it formally follows from Proposition 5.1 that if an *in trans* solution tangle under the PJH framing has fewer than 9 crossings, it must be the [PJH] solution of Figure 0.1.

The proof of Proposition 5.1 breaks down into checking cases of possible tangle diagrams. We focus on the fact that $s_{12} \cup s_{13} = \mathcal{T} - s_{23}$ is the $-1/2$ tangle. Lemma 5.2 shows that each pair of strings must cross at least twice. Hence if an *in trans* solution tangle has less than 10 crossings, $s_{12} \cup s_{13}$ contains at most 5 crossings. Theorems 5.5, 5.7, 5.12, 5.14 handle the cases when $s_{12} \cup s_{13} = 2, 3, 4, 5$, respectively. In each case it is shown that an *in trans* solution tangle with less than 10 crossings can be isotoped to a tangle with 7 crossings. By Corollary 4.5, such a tangle is the PJH tangle. This section holds more generally under normal framing when the *in trans* deletion product is the $(2,2)$ torus link while the remaining deletion products are $(2, L_i)$ torus links where $L_i \geq 4$.

Lemma 5.2. *Let \mathcal{T} be a solution tangle. In any projection of \mathcal{T} , $|s_{ij} \cap s_{ik}| \geq 2$.*

Proof. Assume not. Then $|s_{ij} \cap s_{ik}| = 0$. But then $\ell k(s_{ij} \cup x_{ij}, s_{ik} \cup x_{ik}) = 0$, contradicting Lemma 2.2. \square

Let \mathcal{T} be an *in trans* solution tangle with crossing number less than 10. We assume that s_{23} is the enhancer strand. To simplify notation we set $e = s_{23}$, $\alpha_2 = s_{12}$, $\alpha_3 = s_{13}$. Recall that $\mathcal{T} - e = \alpha_2 \cup \alpha_3$ is the $-1/2$ -tangle.

Assumption 5.3. \mathcal{T} has a projection, in normal form (see the beginning of Section 2), with at most nine crossings. Furthermore, among all such projections, take $\alpha_2 \cup \alpha_3$ to have the fewest crossings.

Remark. We will often blur the distinction between e , α_2 , α_3 and their projections.

We will first prove in Theorem 5.5 that Proposition 5.1 holds when $\alpha_2 \cup \alpha_3$ has exactly two crossings. In this case let R_1, R_2, R_3 be the closures of the complementary regions of

$\alpha_2 \cup \alpha_3$ in Figure 5.1. Note all figures in this section have been rotated by 90 degrees, and thus the tangle $\mathcal{T} - e = -1/2$ is displayed as an integral 2 tangle.

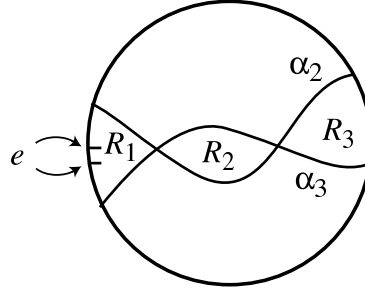


FIGURE 5.1

Lemma 5.4. *If e crosses $R_1 \cap (\alpha_2 \cup \alpha_3)$ fewer than four times then \mathcal{T} can be freely isotoped to eliminate two crossings. Furthermore if $e \cap R_1$ contains only four crossings of \mathcal{T} then we can reduce \mathcal{T} by two crossings unless $e \cap R_1$ is as pictured in Figure 5.2 (up to symmetry).*

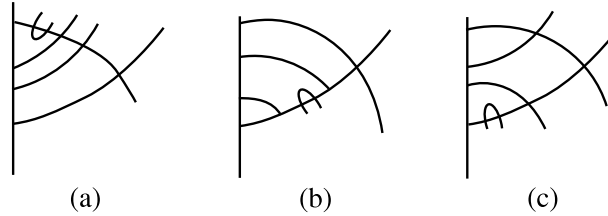


FIGURE 5.2

Proof. Assume e intersects $R_1 \cap (\alpha_2 \cup \alpha_3)$ in fewer than four crossings. By Lemma 5.2, e must cross $R_1 \cap (\alpha_2 \cup \alpha_3)$ exactly twice. Then R_1 writes $\mathcal{T} \cup c_1$ as a disk sum. As $\mathcal{T} \cup c_1$ is a rational 2-string tangle, $e \cap R_1$ must be an integral summand [L, ES1]. But then we can reduce the crossing number by at least two under a free isotopy by removing the crossings in the integral tangle $e \cap R_1$ as well as the two crossings where e intersects

$R_1 \cap (\alpha_2 \cup \alpha_3)$. See Figure 5.3.

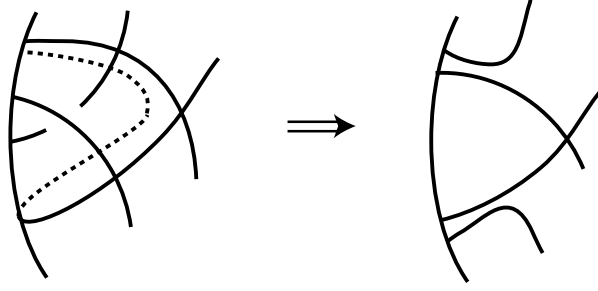


FIGURE 5.3

Thus we assume $e \cap R_1$ must have at least 4 crossings in R_1 with $\alpha_2 \cup \alpha_3$. Assume these are the only crossings of \mathcal{T} in R_1 . Then there are no crossings in $\text{int } R_1$. This allows for two crossing reductions except in the cases pictured in Figure 5.2. See Figure 5.4.

□(Lemma 5.4)

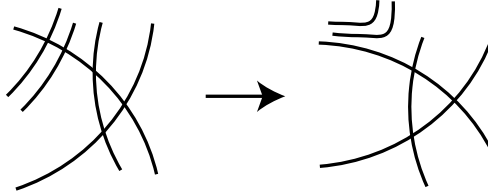


FIGURE 5.4

Theorem 5.5. *Let \mathcal{T} be an in trans solution tangle satisfying Assumption 5.3. Under this projection, assume $\alpha_2 \cup \alpha_3$ has exactly two crossings. Then \mathcal{T} can be freely isotoped to have at most seven crossings.*

Proof. Let R_1, R_2, R_3 be the closures of the complementary regions of $\alpha_2 \cup \alpha_3$ in Figure 5.1.

We divide the proof of Theorem 5.5 into two cases.

Case I: e has 4 intersections in R_1 .

Case II: e has at least 5 intersections in R_1 .

Proof of Case I: R_1 contains exactly 4 crossings (involving e). In this case, there are 3 possible configurations up to symmetry (shown in Figure 5.2) that do not immediately allow a crossing reduction by two in R_1 .

Since there are at most 9 crossings, if e intersects R_2 then $e \cap R_2$ must contribute exactly 2 crossings and $e \cap R_3$ must be empty. But this allows a reduction of two crossings: In case (a) and (b) in Figure 5.2, the two crossing involving α_2 and α_3 can be removed as

shown in Figure 5.5.

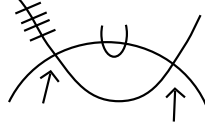


FIGURE 5.5

In case (c) one reduction comes from $\alpha_1 \cap \alpha_2$, the other from $e \cap (\alpha_2 \cup \alpha_3)$ (Figure 5.6).

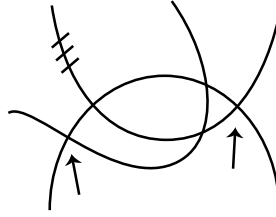


FIGURE 5.6

Thus we take e disjoint from R_2 , and we must have (a) or (b) in Figure 5.7.

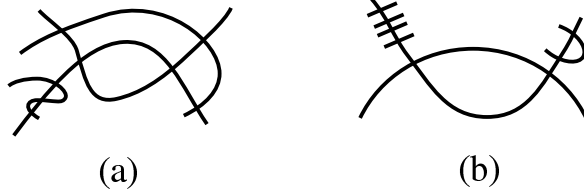


FIGURE 5.7

But (a) gives two crossing reductions and (b) contradicts Lemma 5.2.

Q.E.D. (Case I)

Proof of Case II: Because e must pick up at least two crossings in $R_2 \cup R_3$, (else we can reduce by two crossings), e must have exactly 4 crossings with $(\alpha_2 \cup \alpha_3) \cap R_1$ and exactly 1 self-crossing inside R_1 . This accounts for nine crossings. For subcases 1 and 2, we assume the two crossings are with R_3 — if not, a similar argument works if the two crossings are with R_2 by using the fact that the crossing at R_3 would be reducible.

Let δ_2, δ_3 (in α_2, α_3 , resp.) be the arc components of $[\alpha_2 \cup \alpha_3 - (\alpha_2 \cap \alpha_3)] \cap R_1$.

Subcase 1). $|\delta_2 \cap e| = 2 = |\delta_3 \cap e|$ (intersection here refers to the projection)

Then we may assume we have

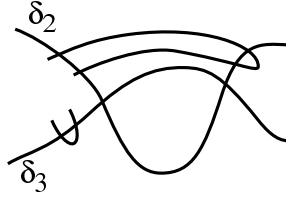


FIGURE 5.8

Since $\text{int } R_1$ has exactly one crossing, the possible cases are

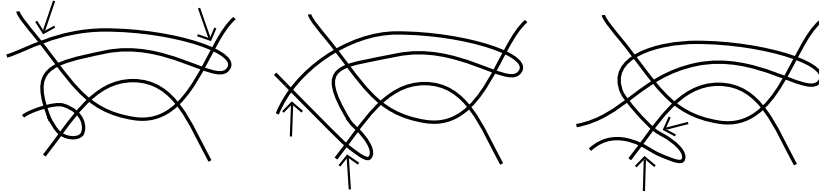


FIGURE 5.9

In each case we can reduce two crossings.

Subcase 2). $|\delta_2 \cap e| = 3$, $|\delta_3 \cap e| = 1$ (case when $|\delta_2 \cap e| = 1$, $|\delta_3 \cap e| = 3$ is similar).

We have two possibilities

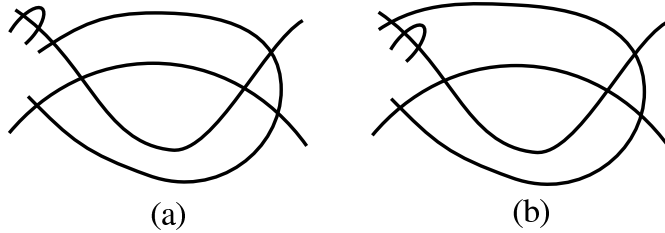


FIGURE 5.10

Recall that R_1 can have only one more crossing in its interior. If this crossing can be reduced, we can reduce two more crossings by case 1. Hence, we assume that this crossing cannot be reduced. Thus we see that both of the cases in Figure 5.10 allow a

reduction of two crossings:

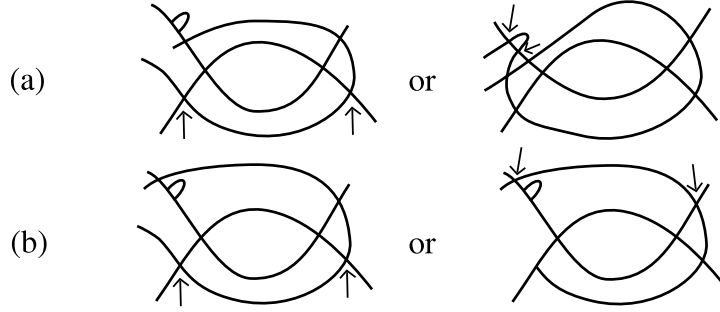


FIGURE 5.11

Subcase 3). $|\delta_2 \cap e| = 4$, $|\delta_3 \cap e| = 0$ (case when $|\delta_2 \cap e| = 0$, $|\delta_3 \cap e| = 4$ is similar).

Recall $|e \cap (R_2 \cup R_3)| = 2$. If $|e \cap R_3| = 2$, then $|e \cap \alpha_3| < 2$, contradicting Lemma 5.2. If $|e \cap R_2| = 2$, then we can remove the two crossings of $\alpha_2 \cap \alpha_3$.

Subcases (1)–(3) exhaust all possibilities, showing a reduction in crossing number by two in Case II.

Q.E.D. (Case II)

This finishes the proof to Theorem 5.5.

□(Theorem 5.5)

Definition 18. α_i has a trivial self-intersection w.r.t. α_j if α_i has a self-intersection such that the subarc of α_i connecting the double points is disjoint from α_j , $\{i, j\} = \{2, 3\}$.

Lemma 5.6. *If \mathcal{T} is an in trans solution tangle satisfying Assumption 5.3 and α_i has a trivial self-intersection w.r.t. α_j for $\{i, j\} = \{2, 3\}$, then we can reduce \mathcal{T} by two crossings.*

Proof. Assume α_2 has a trivial self-intersection w.r.t. α_3 , and let $\delta \subset \alpha_2$ be the subarc connecting its double points. As $|\alpha_2 \cap \alpha_3|$ is minimal, Figure 5.12 shows that we may assume $|\delta \cap e| \geq 4$.

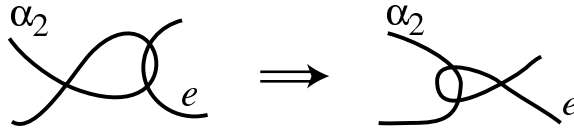


FIGURE 5.12

By Lemma 5.2, $|\alpha_2 \cap \alpha_3| \geq 2$ and $|e \cap \alpha_3| \geq 2$. Thus $|\delta \cap e| = 4$, $|\alpha_2 \cap \alpha_3| = 2$, $|e \cap \alpha_3| = 2$ and α_2 has a self crossing, accounting for all nine crossings. Let $\alpha'_2 = \alpha_2 - \text{int}(\delta)$. Let R_1, R_2, R_3 be the closures of the complementary regions of $\alpha'_2 \cup \alpha_3$ as in Figure 5.1. Then

$|e \cap \partial R_1| \geq 2$ and $|e \cap (\partial R_2 \cup \partial R_3)| \geq 2$, otherwise we can reduce by two the number of crossings. Thus $|e \cap (\alpha_2 \cup \alpha_3)| \geq 8$. Because $|\alpha_2 \cap \alpha_3| \geq 2$, we have too many crossings. \square

Theorem 5.7. *Let \mathcal{T} be an in trans solution tangle satisfying Assumption 5.3. If $\alpha_2 \cup \alpha_3$ contributes three crossings to \mathcal{T} (including self-crossings), then \mathcal{T} can be freely isotoped to have at most seven crossings.*

Proof. Let \mathcal{T} be such an in trans solution tangle. Then α_3 , say, must have a self-intersection which we may assume is not trivial w.r.t. α_2 . Thus $\alpha_2 \cup \alpha_3$ must be as in Figure 5.13, with R_1, R_2 complementary components of $\alpha_2 \cup \alpha_3$, R_1 containing the endpoints of e , and $\delta_1, \delta_2, \dots, \delta_8$ the arc components of $\alpha_2 \cup \alpha_3 - (\alpha_2 \cap \alpha_3)$.

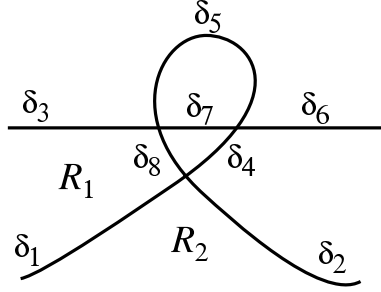


FIGURE 5.13

Claim 5.8. *If $|e \cap (R_1 \cap (\alpha_2 \cup \alpha_3))| < 4$, then \mathcal{T} can be reduced by two crossings.*

Proof. We may assume that $|e \cap (R_1 \cap (\alpha_2 \cup \alpha_3))| = 2$. Then a copy of ∂R_1 writes $\mathcal{T} \cup c_1$ as a disk sum. Since $\mathcal{T} \cup c_1$ is a rational tangle, one of the summands must be integral w.r.t. to the disk. This must be the left-hand side, $R_1 \cap e$. After a free isotopy we may take this to be $\frac{0}{1}$. Hence we can take e to have no self-crossings in R_1 .

Let δ_1, δ_2 be as pictured in Figure 5.13. If $|e \cap \delta_1| = 2$, then we can freely isotop away two crossings. If $|e \cap \delta_1| = 1$, then $|e \cap \delta_2| \geq 3$ (else we can reduce two crossings in R_2). Since $|e \cap \alpha_2| \geq 2$ by Lemma 5.2, $|e \cap \alpha_2|$ must be two, accounting for all intersections. That is, if $|e \cap \delta_1| = 1$ we are as in Figure 5.14, where we can reduce by two crossings.

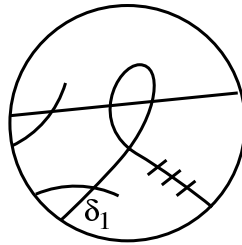


FIGURE 5.14

Thus we assume e is disjoint from δ_1 .

Similarly we show that e is disjoint from δ_3 (see Figure 5.13). If $|e \cap \delta_3| = 2$, then we can reduce by two crossings in R_1 . So assume $|e \cap \delta_3| = 1$. If $e \cap \delta_2$ is empty we can reduce two crossings (the self-intersection and $e \cap \delta_3$), so $|e \cap \delta_2| \geq 2$. The only possibility is shown now in Figure 5.15, which we can reduce by two crossings.

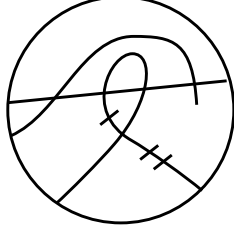


FIGURE 5.15

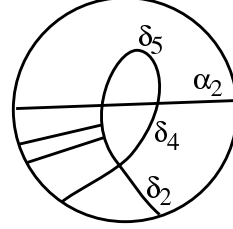


FIGURE 5.16

So we assume e is disjoint from arcs δ_1 and δ_3 in ∂R_1 . See Figure 5.16.

Now $|e \cap \alpha_2| \geq 2$ by Lemma 5.2, and $|e \cap \delta_2| \geq 2$ (else we can reduce two crossings). This accounts for all nine crossings. But we must also have a crossing between e and $\delta_4 \cup \delta_5$. \square

Claim 5.9. e must intersect δ_1 .

Proof. By Claim 5.8, we may assume $|e \cap (R_1 \cap (\alpha_1 \cup \alpha_3))| \geq 4$. Label the arc components of $\alpha_2 \cup \alpha_3 - (\alpha_2 \cap \alpha_3)$ as in Figure 5.13. Assume e is disjoint from δ_1 . It cannot also be disjoint from δ_2 , otherwise we can eliminate the crossing at $\delta_1 \cap \delta_2$ and argue as in Case I of Theorem 5.5. Thus e must intersect δ_2 exactly twice, thereby accounting for all crossings. But the crossings of e at δ_2 lead to additional crossings. \square

Claim 5.10. \mathcal{T} can be reduced by two crossings if $|e \cap (R_1 \cap (\alpha_2 \cup \alpha_3))| < 6$.

Proof. By Claim 5.8, we may assume $|e \cap (R_1 \cap (\alpha_1 \cup \alpha_3))| = 4$.

Subclaim 5.11. $e \cap (\delta_6 \cup \delta_7)$ is non-empty.

Proof. Suppose $e \cap (\delta_6 \cup \delta_7)$ is empty. Then $|e \cap \delta_3| = 2$ by Lemma 5.2. If e crosses δ_5 then it must cross twice, accounting for all crossings of \mathcal{T} . Then there are no crossings in $\text{int } R_1$. Since $|e \cap \delta_1| > 0$ and $|e \cap \delta_3| = 2$, we have two crossing reductions in R_1 . Thus e is disjoint from δ_5 .

Similarly e must not cross δ_2 . If $|e \cap \delta_2| \neq 0$, then there can be no crossings in $\text{int } R_1$. Since $|e \cap \delta_1| > 0$ and $|e \cap \delta_3| = 2$, we see the crossing reductions for \mathcal{T} . Since e does not cross δ_2 , but does cross δ_1 , e must cross δ_1 twice. Hence e also does not cross δ_8 .

Thus we assume e does not cross $\delta_2, \delta_5, \delta_6, \delta_7$, or δ_8 . As the 2-string tangle α_2, α_3 forms a two crossing tangle, we see that the crossings between α_2 and α_3 may be reduced in \mathcal{T} . $\square(5.11)$

Assume first that e crosses δ_7 . Then e must cross $\delta_5 \cup \delta_7$ twice, accounting for all crossings. Then e does not cross δ_2 and crosses δ_1 exactly two times. These crossings can be reduced.

Thus e crosses δ_6 . If e does not cross δ_2 then we again see two crossings at δ_1 that can be reduced. If e crosses δ_2 then it crosses it once, accounting for all crossings. Thus e crosses each of δ_1 and δ_3 an odd number of times and has no self-crossings in int R_1 . Enumerating the possibilities one sees that we can reduce the crossings of e at δ_3, δ_6 or at δ_1, δ_2 .

This finishes the proof of Claim 5.10. $\square(5.10)$

By Claim 5.10 we may assume $|e \cap R_1 \cap (\alpha_2 \cup \alpha_3)| = 6$. This accounts for all crossings of \mathcal{T} . By Lemma 5.2, $|e \cap \delta_3| \geq 2$. As all crossings are accounted for, two of the crossings of e with $\delta_1 \cup \delta_3$ can be eliminated by a free isotopy.

Q.E.D. (Theorem 5.7)

\square

Theorem 5.12. *Let \mathcal{T} be an in trans solution tangle satisfying assumption 5.3. If $\alpha_2 \cup \alpha_3$ has four crossings (including self-crossings), then there is a free isotopy of \mathcal{T} reducing it to at most seven crossings.*

Proof. Assume \mathcal{T} is as hypothesized. By Lemma 5.6, $\alpha_2 \cup \alpha_3$ has no trivial loops and we enumerate the possibilities for $\alpha_2 \cup \alpha_3$ in Figure 5.17 where R_1 is the closure of the (planar) complementary region of $\alpha_1 \cup \alpha_2$ containing the ends of e and where δ_1, δ_2 are

the extremal arc components of $\alpha_2 \cup \alpha_3 - (\alpha_2 \cap \alpha_3)$ in R_1 .

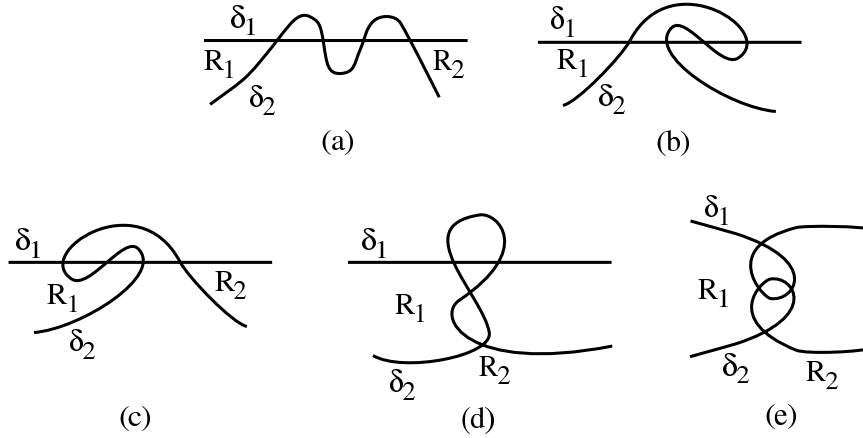


FIGURE 5.17

Lemma 5.13. *With \mathcal{T} as in the hypothesis of Theorem 5.12, if e contains a self-crossing then that self-crossing appears in R_1 .*

Proof. Assume a self-crossing appears in a complementary region $R \neq R_1$ of $\alpha_2 \cup \alpha_3$. Since $|\alpha_2 \cap \alpha_3| = 4$, $|e \cap \alpha_2| = 2$, $|e \cap \alpha_3| = 2$, e can have at most one self-crossing. Hence R has exactly 5 crossings involving e : four from e crossing $\alpha_2 \cup \alpha_3$ and one self-crossing. By Lemma 5.2, e must cross α_2 twice and α_3 twice in R . Exactly one pair of these crossings must be in a component of $\alpha_2 \cup \alpha_3 - (\alpha_2 \cap \alpha_3)$ shared with R_1 (all crossings are accounted for). If this component is δ_1 or δ_2 we may reduce by two crossings. So we assume this pair is in a different component. Looking at the possibilities of Figure 5.17, we immediately rule out (a) and (b). In cases (c), (d), and (e), we can reduce two crossings of $\alpha_2 \cup \alpha_3$ since we have accounted for all crossings (for case (d), note e must cross each of α_2 and α_3 twice in R).

□

We continue the proof of Theorem 5.12.

Case I: e crosses $R_1 \cap (\alpha_2 \cup \alpha_3)$ exactly twice. If both crossings are in $\delta_1 \cup \delta_2$, then we can reduce by two crossings. This rules out configurations (a),(b) of Figure 5.17. If \mathcal{T} has nine crossings, then one must be a self-crossing. By Lemma 5.13 it must occur in R_1 and hence can be untwisted to reduce the crossing number by one. Thus we assume \mathcal{T} has only 8 crossings. Hence e must be disjoint from $\delta_1 \cup \delta_2$. In cases (c), (d), and (e), e must then be disjoint from the region labelled R_2 . But then we can reduce the crossing at R_2 . □(Case I)

Case II: e crosses $R_1 \cap (\alpha_2 \cup \alpha_3)$ **four times**. If \mathcal{T} has nine crossings then one must be a self-crossing of e . By Lemma 5.13, the self-crossing occurs in R_1 . Thus, whether \mathcal{T} has eight or nine crossings, all crossings of \mathcal{T} involving e lie in R_1 . By Lemma 5.2, two of the crossings of e are with α_2 and two with α_3 . Looking at Figure 5.17, we see that e must have exactly two crossings with δ_i for $i = 1$ or 2 (in cases (c) and (e) we could otherwise reduce by two crossings). Either we can reduce by two crossings or near δ_i we have Figure 5.18.

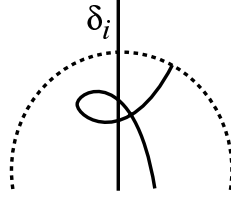


FIGURE 5.18

This writes $\mathcal{T} \cup_{C_1}$ as a disk sum. As $\mathcal{T} \cup_{C_1}$ is integral w.r.t. the disk slope, each summand is integral w.r.t. to the disk slope. But this means we can eliminate the crossings at δ_i by a free isotopy of \mathcal{T} . \square (Case II)

Q.E.D. (Theorem 5.12)

Theorem 5.14. *Let \mathcal{T} be an in trans solution tangle satisfying assumption 5.3. If $\alpha_2 \cup \alpha_3$ has five crossings (including self-crossings), then there is a free isotopy of \mathcal{T} reducing it to at most seven crossings.*

Proof. Let \mathcal{T} be such a tangle. WLOG assume α_2 has at most one self-intersection. By Lemma 5.2 e must cross each of α_2, α_3 exactly twice. Since e can contribute at most 4 crossings this accounts for all crossings coming from e . In particular, e has no self-crossings.

Case I. α_2 crosses α_3 twice.

We have three possibilities as shown in Figure 5.19 (Lemma 5.6), where R_1 is the complementary region of $\alpha_2 \cup \alpha_3$ containing the ends of e (ℓ is discussed below).

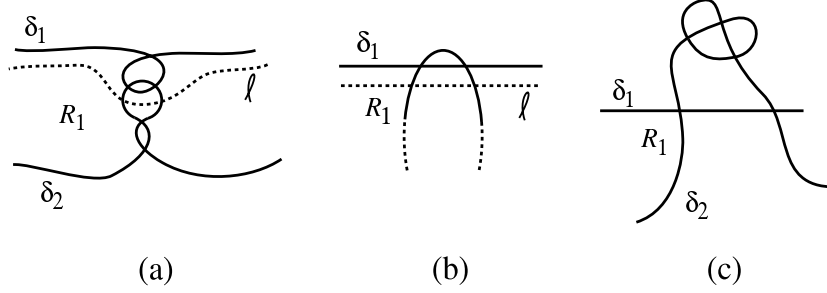


FIGURE 5.19

In case (c) we may reduce the crossings of \mathcal{T} by two (\mathcal{T} has no local knots, hence $|e \cap (\delta_1 \cup \delta_2)| = 2$). So we restrict our attention to (a) and (b) and consider the arc ℓ in Figure 5.19. Since $|e \cap \alpha_2| = 2$, ℓ intersects e twice. Hence $e \cup \ell$ is as in Figure 5.20, where e', e'' are components of $e - \ell$.

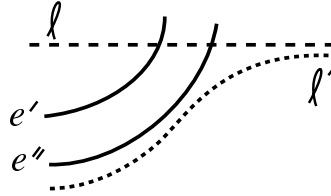


FIGURE 5.20

Let ℓ' be the arc pictured in Figure 5.20, consisting of e'' and part of ℓ .

Claim 5.15. $|\ell' \cap \alpha_3| = 2$.

Proof. $|\ell' \cap \alpha_3|$ is even and at least 2, since the endpoints of α_3 are below ℓ' . If $|\ell' \cap \alpha_3| \geq 4$, then $|e'' \cap \alpha_3| = 2 = |(\ell' - e'') \cap \alpha_3|$. Going back to Figure 5.19 we see we can eliminate the crossings of e and α_2 . $\square(5.15)$

By Claim 5.15, ℓ' writes $\mathcal{T} \cup c_2$ as a disk sum. By Lemma 2.1, if \mathcal{T} is a normal form solution tangle, $\mathcal{T} \cup c_2$ is the $-1/4$ tangle. As the crossing number of the summand below ℓ' is at most 3, the tangle below ℓ' is integral w.r.t. the disk slope — allowing us to eliminate the crossings there. Thus there is at most one crossing below ℓ' . Now we can eliminate two crossings from \mathcal{T} , where α_3 crosses e'' or α_2 near where α_3 crosses ℓ' . $\square(\text{Case I})$

Case II. α_2 crosses α_3 four times.

WLOG assume α_2 has no self-intersections and α_3 only one. Then $\alpha_2 \cup \alpha_3$ must be one of the cases in Figure 5.21.

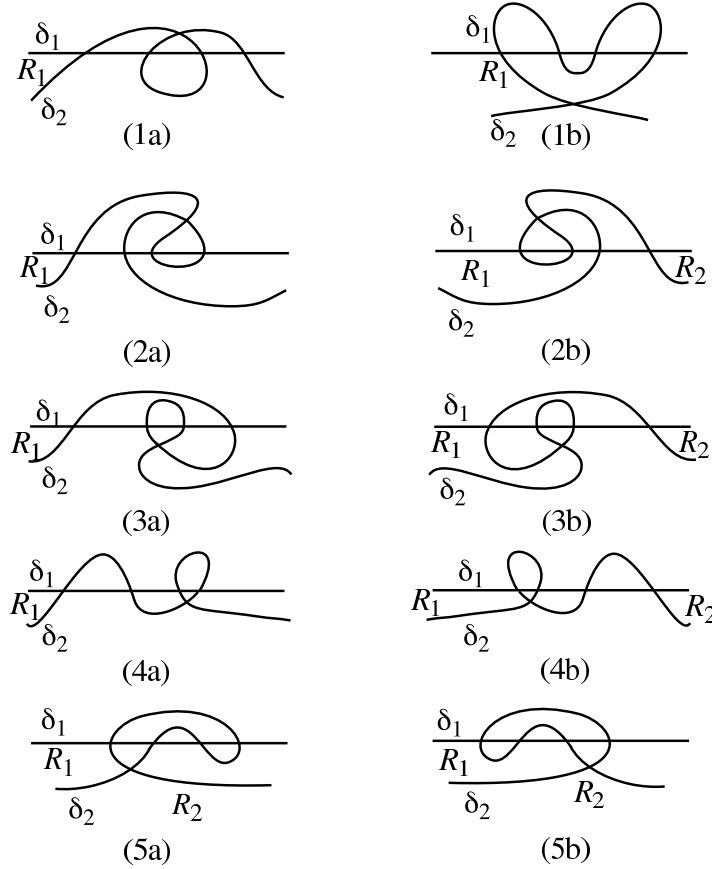


FIGURE 5.21

Claim 5.16. $|e \cap (\delta_1 \cup \delta_2)| \leq 1$.

Proof. Assume $|e \cap (\delta_1 \cup \delta_2)| \geq 2$. If $|e \cap R_1 \cap (\alpha_2 \cup \alpha_3)| \leq 2$, then the crossings at $\delta_1 \cup \delta_2$ can be eliminated. So assume $|e \cap R_1 \cap (\alpha_2 \cup \alpha_3)| = 4$, accounting for all crossings of e . Then $|e \cap \delta_i| = 2$ for some $i = 1, 2$, and we can reduce these crossings. $\square(5.16)$

Claim 5.16 eliminates cases (1a), (2a), (3a), (4a). If $|e \cap \delta_i| = 1$ then it must give rise to a reducible crossing in R_1 . In cases (2b), (3b), (4b) we could then reduce also the crossing at R_2 . In these cases then we assume e disjoint from $\delta_1 \cup \delta_2$. By inspection we now see we can reduce by two crossings ($|e \cap (\alpha_2 \cup \alpha_3)| = 4$).

We are left with (1b), (5a) and (5b). If $|e \cap \delta_2| = 1$, then we can eliminate two crossings at $e \cap R_2$. If $|e \cap \delta_1| = 1$, then we can eliminate this crossing and the self-crossing of α_3 . With $|e \cap \alpha_2| = 2 = |e \cap \alpha_3|$ and $e \cap (\delta_1 \cup \delta_2)$ empty, we see that in all possibilities we

can eliminate two crossings from \mathcal{T} .

Q.E.D. (Theorem 5.14)

REFERENCES

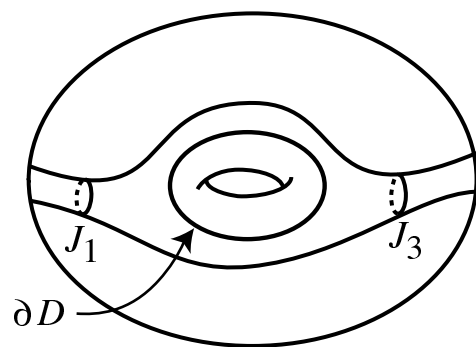
- [BM] T Baker, K. Mizuuchi, *DNA-promoted assembly of the active tetramer of the Mu transposase*, Genes Dev. **6**(11) (1992) 2221–32.
- [BSC] J. Bath, D.J. Sherratt and S.D. Colloms, *Topology of Xer recombination on catenanes produced by lamda integrase*, J. Mol. Biol. **289**(4) (1999), 873–883.
- [BL] S. Bleiler and R. A. Litherland, *Lens spaces and Dehn surgery*, Proceedings of the American Mathematical Society **107**(4) (1989), 1127–1131.
- [BV] D. Buck, C. Verjovsky Marcotte, *Tangle solutions for a family of DNA-rearranging proteins*, Math. Proc. Camb. Phil. Soc. **139**(1) (2005), 59–80.
- [C1] H. Cabrera-Ibarra, *On the classification of rational 3-tangles*, Journal of Knot Theory and its Ramifications **12** (2003), 921–946.
- [C2] H. Cabrera-Ibarra, *Results on the classification of rational 3-tangles*, Journal of Knot Theory and its Ramifications **13** (2004), 175–192.
- [CG] A. J. Casson, C. McA. Gordon *Reducing Heegaard splittings*. Topology Appl. **27** (1987), no. 3, 275–283.
- [CH] G. Chaconas and R. M. Harshey, *Transposition of phage Mu DNA*. In Mobile DNA II. N. L. Craig, R. Craigie, M. Gellert, and A. M. Lambowitz (ed), (2002) pp 384–402, American Society for Microbiology.
- [CLW] G. Chaconas, B.D. Lavoie, and M.A. Watson, *DNA transposition: jumping gene machine, some assembly required*, Curr. Biol. **6** (1996), 817–820.
- [CBS] S.D. Colloms, J. Bath and D.J. Sherratt, *Topological selectivity in Xer site-specific recombination*, Cell **88** (1997), 855–864.
- [CGLS] M. Culler, C. Gordon, J. Luecke, P.B. Shalen *Dehn surgery on knots.*, Bull. Amer. Math. Soc. (N.S.) **13** (1985), no. 1, 43–45.
- [D] I. Darcy, *Biological distances on DNA knots and links: Applications to Xer recombination*, Journal of Knot Theory and its Ramifications **10** (2001), 269–294.
- [D1] I. K. Darcy, A. Bhutra, J. Chang, N. Druivenga, C. McKinney, R. K. Medikonduri, S. Mills, J. Navarra Madsen, A. Ponnusamy, J. Sweet, T. Thompson, *Coloring the Mu Transpososome*, BMC Bioinformatics, **7**, (2006), Art. No. 435.
- [DMBK] P. L. Deininger, J. V. Moran, M. A. Batzer, H. H. Kazazian Jr., *Mobile elements and mammalian genome evolution*, Curr Opin Genet Dev. 2003 **13**(6) (2003), 651–8.
- [EE] J. Emert, C. Ernst, *N-string tangles*, Journal of Knot Theory and its Ramifications **9** (2000), 987–1004.
- [ES1] C. Ernst, D. W. Sumners, *A calculus for rational tangles: applications to DNA recombination*, Math. Proc. Camb. Phil. Soc. **108** (1990), 489–515.
- [ES2] C. Ernst, D. W. Sumners, *Solving tangles equations arising in a DNA recombination model*, Math. Proc. Camb.Phil. Soc. **126** (1999), 23–36.
- [GEB] I. Goldhaber-Gordon, M.H. Early, and T.A. Baker, *MuA transposase separates DNA sequence recognition from catalysis*, Biochemistry **42** (2003), 14633–14642.
- [G] C. Gordon *On the primitive sets of loops in the boundary of a handlebody*, Topology and Appl. **27** (1987), 285–299.
- [GBJ] I. Grange, D. Buck, and M. Jayaram, *Geometry of site alignment during int family recombination: antiparallel synapsis by the FLP recombinase*, J. Mol. Biol. **298** (2000), 749–764.
- [GGD] F. Guo, D.N. Gopaul, and G.D. van Duyne, *Structure of Cre recombinase complexed with DNA in a site-specific recombination synapse*, Nature **389** (1997), 40–46.

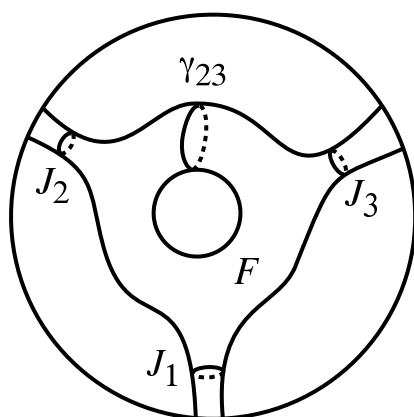
- [HJ] R. Harshey and M. Jayaram, *The mu transpososome through a topological lens*, Crit Rev Biochem Mol Biol. **41**(6) (2006), 387–405.
- [HS] M. Hirasawa and K. Shimakawa, *Dehn surgeries on strongly invertible knots which yield lens spaces*, PAMS **128** (2000), no. 11, 3445–3451.
- [J] W. Jaco, *Adding a 2-handle to 3-manifolds: an application to Property R*, PAMS **92** (1984), 288–292.
- [KBS] E. Kilbride, M.R. Boocock, and W.M. Stark, *Topological selectivity of a hybrid site-specific recombination system with elements from Tn3 res/resolvase and bacteriophage PL lox P/Cre*, J. Mol. Biol. **289** (1999), 1219–1230.
- [KMOS] P. Kronheimer, T. Mrowka, P. Ozsvath, Z. Szabo *Monopoles and lens space surgeries*, Ann. of Math. (2) **165**(2) (2007), 457–546.
- [L] W. B. R. Lickorish, *Prime knots and tangles*, Trans. Amer. Math. Soc. **267**(1) (1981), 321–332.
- [MBM] M. Mizuuchi, T. A. Baker, K. Mizuuchi, *Assembly of the active form of the transposase-Mu DNA complex: a critical control point in Mu transposition*, Cell **70**(2) (1992) 303–11.
- [PJH] S. Pathania, M. Jayaram, and R. Harshey, *Path of DNA within the Mu Transpososome: Transposase interaction bridging two Mu ends and the enhancer trap five DNA supercoils*, Cell **109** (2002), 425–436.
- [PJH2] S. Pathania, M. Jayaram, and R. Harshey, *A unique right end-enhancer complex precedes synapsis of Mu ends: the enhancer is sequestered within the transpososome throughout transposition*, EMBO J. **22**(14) (2003), 3725–36.
- [S] D. Sankoff, *Rearrangements and chromosomal evolution*, Curr Opin Genet Dev. **13**(6) (2003) 583–7.
- [Sch] M. Scharlemann, *Outermost forks and a theorem of Jaco* Proc. Rochester Conf., AMS Contemporary Math. Series **44** (1985), 189–193.
- [ST] M. Scharlemann and A. Thompson, *Detecting unknotted graphs in S^3* , J. Differential Geom. **34** (1991) 539–560.
- [SECS] D. W. Sumners, C. Ernst, N.R. Cozzarelli, S.J. Spengler *Mathematical analysis of the mechanisms of DNA recombination using tangles*, Quarterly Reviews of Biophysics **28** (1995).
- [T] A. Thompson, *A polynomial invariant of graphs in 3-manifolds*, Topology **31** (1992) 657–665.
- [VCS] M. Vazquez, S.D. Colloms, D.W. Sumners, *Tangle analysis of Xer recombination reveals only three solutions, all consistent with a single three-dimensional topological pathway*, J. Mol. Biol. **346** (2005), 493–504.
- [VS] M. Vazquez, D. W. Sumners, *Tangle analysis of Gin site-specific recombination*, Math. Proc. Camb. Phil. Soc. **136** (2004), 565–582.
- [VDL] A.A. Vetcher, A. Y. Lushnikov, J. Navarra-Madsen, R. G. Scharein, Y. L. Lyubchenko, I. K. Darcy, S. D. Levene, *DNA topology and geometry in Flp and Cre recombination*, J Mol Biol. **357**(4) (2006), 1089–104.
- [Wu1] Y. Q. Wu, *A generalization of the handle addition theorem*, PAMS **114** (1992), 237–242.
- [Wu2] Y. Q. Wu, *On planarity of graphs in 3-manifolds*, Comment. Math. Helv. **67** (1992) 635–64.
- [Wu3] Y. Q. Wu, *The classification of nonsimple algebraic tangles*, Math. Ann. **304**(3) (1996), 457–480.
- [YJPH] Z. Yin, M. Jayaram, S. Pathania, and R. Harshey, *The Mu transposase interwraps distant DNA sites within a functional transpososome in the absence of DNA supercoiling*, J Biol Chem. **280**(7) (2005), 6149–56.
- [YJH] Z. Yin, A. Suzuki, Z. Lou, M. Jayaram, and R. Harshey, *Interactions of phage Mu enhancer and termini that specify the assembly of a topologically unique interwrapped transpososome*, J Mol Biol. **372**(2) (2007), 382–96.

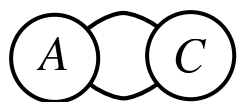
Isabel K. Darcy, Department of Mathematics, University of Iowa, Iowa City, IA 52242
E-mail: idarcy@math.uiowa.edu
URL: <http://www.math.uiowa.edu/~idarcy>

John Luecke, Department of Mathematics, University of Texas at Austin, Austin, TX 78712
E-mail: luecke@math.utexas.edu
URL: <http://www.ma.utexas.edu/~luecke/>

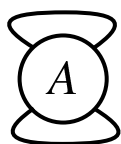
Mariel Vazquez, San Francisco State University Department of Mathematics, 1600 Holloway Ave, San Francisco, CA 94132
E-mail: mariel@math.sfsu.edu
URL: <http://math.sfsu.edu/vazquez/>



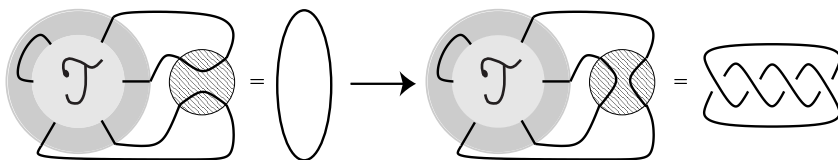




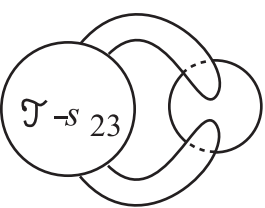
$A + C$



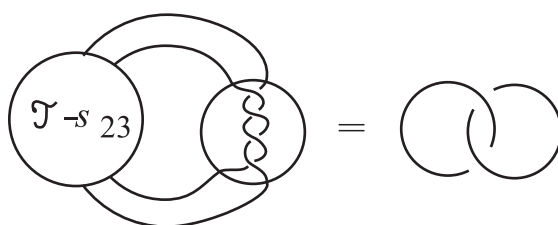
$N(A)$



$N(\mathcal{T} + 0/1) = N(1/0) \rightarrow N(\mathcal{T} + 1/0) = N(4/1)$



unknot



Hopflink